Population structure and reproduction of the alvinocaridid shrimp Rimicaris exoculata on the Mid-Atlantic Ridge: Variations between habitats and vent fields

Ivan Hernandez, Marie-Anne Cambon-Bonavita, Jozee Sarrazin, Florence Pradillon

Population structure and reproduction of the alvinocaridid shrimp *Rimicaris exoculata* on the Mid-Atlantic Ridge: variations between habitats and vent fields

Iván Hernández-Ávila [a, 1, *], Marie-Anne Cambon-Bonavita [b], Jozée Sarrazin [a], Florence Pradillon [a, *]

[a] Ifremer, REM/EEP, Laboratoire Environnement Profond, F 29280 Plouzané, France.

[b] Univ Brest, Ifremer, CNRS, Laboratoire de Microbiologie des Environnements Extrêmes, F 29280 Plouzané, France.

*Corresponding author: ihernandez@pampano.unacar.mx, florence.pradillon@ifremer.fr

[1] Present address: Facultad de Ciencias Naturales, Universidad Autónoma del Carmen, Ciudad del Carmen, Mexico

ORCID :

IHA : 0000-0002-6722-5226

MACB : 0000-0002-4076-0472

JS : 0000-0002-5435-8011

FP : 0000-0002-6473-6290

Abstract

The shrimp *Rimicaris exoculata* is the most conspicuous component of vent communities developing around hydrothermal fluid emissions below 2000 m on the northern Mid-Atlantic Ridge (nMAR). Its high genetic connectivity suggests a remarkable ability to produce dispersing larval stages. However, so far brooding females have been rarely observed and reproduction remained enigmatic. Spatially complex population structures related to the heterogeneity of local habitat conditions are described for many vent species, this information being fundamental to gain a better understanding of their life history. Here our aim was to assess such complexity along with reproductive development in *R. exoculata* populations within two vent fields, TAG and Snake Pit (3620m and 3470m depth respectively). We compared samples collected in January-February 2014 among visually distinct assemblages with different degrees of exposure to vent fluids. Dense aggregations located near active venting included mostly females and immature individuals, while inactive peripheries harbored low density assemblages of large males. Small juveniles gathering around low temperature diffusions belonged to another species, *Rimicaris chacei*. One third of the sexually mature females were ovigerous at the two vent fields during our sampling period, with lower fecundities and egg sizes in the TAG population. Overall, the observed shrimp distribution patterns were consistent across both vent fields, although a high degree of heterogeneity in population structure was observed locally within dense aggregations, probably reflecting micro-scale variations in environmental conditions. Our results thus highlight spatially complex population structures where *R. exoculata* females brood eggs within dense aggregations exposed to vent fluids, while peripheral inactive areas may be important mating grounds for adults. In addition, we suggest temporal variability in reproductive activity, increasing in the winter season, which questions potential seasonality in a deep-sea species.

Key words: Life history, population structure, reproduction, *Rimicaris exoculata*, habitat variability, hydrothermal vents.

1. Introduction

At deep-sea hydrothermal vents, the persistence of endemic species at regional scale depends on their ability to disperse and colonize their extremely patchy and locally dynamic habitat. High levels of genetic connectivity between spatially distant vent populations have been observed for many of the visually dominant species (e.g. Thaler et al. 2011, Teixeira et al. 2012, Beedessee et al. 2013). More generally, vent communities are expected to exhibit attributes of resilience facing environmental instability, rooted in the fact that they thrive in naturally highly dynamic habitats (Van Dover, 2014). However, how they would cope with additional challenges caused by human activities in the deep-sea remains difficult to assess because we still lack knowledge on fundamental aspects of their life cycle, demographic connectivity and underlying colonization mechanisms (Van Dover et al. 2018).

The complex and dynamic nature of vent systems generates local patchiness in physico-chemical conditions which influences composition of communities at different temporal and spatial scales (Sarrazin et al. 1997, 2015, Desbruyères et al. 2000, 2001, Cuvelier et al. 2009, 2014). At the species level, population densities and structures are also influenced by local conditions, resulting in spatio-temporal variations. Life stages of a species may occupy different areas characterized by contrasting environmental features at the scale of a single edifice (Cuvelier et al. 2011, Nye et al. 2013, Marsh et al. 2015, Husson et al. 2017). Segregation of juveniles in specific areas were observed in *Bathymodiolus azoricus* mussels (Cuvelier et al. 2009, 2011) and *Rimicaris exoculata* shrimps (Shank et al. 1998), two species dominating vent communities along the northern Mid Atlantic Ridge (nMAR). In the case of *B. azoricus*, spatial segregation was related to the degree of exposure to vent fluids, juveniles being in areas with lower hydrothermal influence (Cuvelier et al. 2011, Husson et al. 2017). Segregation in different habitats according to sex or reproductive status (e.g. brooding females) was also reported in vent decapods (Nye et al. 2013, Marsh et al. 2015). In addition, the chaotic mixing of vent effluents with seawater as well as tidal

71 forcing generate further variability in populations on short temporal scales (Copley et al. 1999).
72 Thus, the interplay between habitat variability and the life cycle of vent species, in which
73 physiological and resource requirements differ with developmental stages, may result in complex
74 population structures. Such complexity must be addressed to better understand vent species life
75 history.

76 On the nMAR, the alvinocarid shrimp *Rimicaris exoculata* (Williams and Rona, 1986) lives
77 close to vent fluid emissions in dense aggregations of thousands of individuals per square meter
78 (Segonzac et al. 1993, Copley et al. 1997, 2007, Gebruk et al. 2000). Its population biology could
79 thus have important implications for the structure, biomass and resilience of the local communities
80 (Gebruk et al. 1997, Desbruyères et al. 2000, 2001). Many aspects of its biology have been
81 investigated (Zbinden and Cambon-Bonavita, 2020), including trophic dependency on bacterial
82 symbionts at the adult stage (Ponsard et al. 2013), regulation of the symbiotic association along
83 the host's life cycle (Corbari et al. 2008, Le Bloa et al. 2020), thermal tolerance (Ravaux et al.
84 2019) as well as sensory abilities (Zbinden et al. 2017, Ravaux et al. 2021). However, population
85 structure and reproduction of *R. exoculata* are less well understood, and available information is
86 often based on single or pooled samples, or on preliminary analyses (e.g. Gebruk et al. 1997,
87 2000, Vereshchaka, 1997). Striking variations in shrimp densities at the TAG and Broken Spur
88 vent fields were related to the availability of substratum exposed to hydrothermal fluids (Copley
89 et al. 1997, 1999), but accompanying variations in population structures were never
90 characterized. Population samples collected at various MAR vent fields showed female-biased
91 sex ratios (Shank et al, 1998), but the association of such bias with a particular habitat or to
92 temporal variations was not evaluated. Habitats located at the base of vent edifices were
93 suggested to serve as nurseries (Gebruk et al. 2000, Komai and Segonzac 2008), and patches
94 of juveniles have also been reported in adult aggregations (Shank et al. 1998, Gebruk et al. 2000,
95 Copley et al. 2007), but their size structure was not defined. Finally, brooding females were

virtually absent from studied populations in different vent fields (Williams and Rona, 1986, Gebruk et al. 1997, Ramirez-Llodra et al. 2000, Copley et al. 2007), except at Logatchev in March 2007 (Gebruk et al. 2010, Guri et al. 2012), which questions their spawning strategy.

In January-February 2014, we explored *R. exoculata* populations from two nMAR vent fields, TAG and Snake Pit. Striking spatial variations in densities of adults and juveniles, similar to those reported in previous studies, and many brooding females were observed. We hypothesized that the visually contrasting shrimp assemblages reflected differences in population structures and habitat conditions. The objectives of the present study are: 1) to compare population structures and local environmental conditions between visually distinct shrimp assemblages, 2) to evaluate regional scale variation by comparing visually similar shrimp assemblages across vent fields, as well as local heterogeneity by comparing randomly collected samples of the same type of assemblage within a single field, and 3) to assess the frequency and distribution of brooding females in the different assemblage types, as well as their fecundities and synchrony to better understand the spawning strategy of the species. This allows us to propose a scenario depicting interactions of shrimps with their conspecifics and their environment at different life stages, and provide clues on some aspects of their reproductive behavior.

2. Material and Methods

2.1. Sampling

Rimicaris exoculata were collected at the TAG (26°08.2'N, 44°49.5'W, 3620 m depth) and Snake Pit (SP, 23°22.1'N 44°57.1'W, 3470 m depth) vent fields on the nMAR (Fig. 1A) during the BICOSE cruise (DOI: 10.17600/14000100) from January 10th to February 11th, 2014. The two vent fields are separated by 300 km of oceanic ridge and a major transform fault (Kane Fracture) shifting its axis by 150 km. Fourteen spatially discrete samples were collected from shrimp assemblages at both vent fields. At TAG, 3 samples were collected in dense shrimp aggregations

swarming on Active Mound (Table 1, Fig. 1B&D, Fig. S1F-H Appendix B) and 2 samples were collected in aggregations of small red alvinocaridid juveniles at the base of the mound, which are herein called “nurseries” (Table 1, Fig. 1F, Fig. S2D-E Appendix B). Additionally, 3 other samples were collected at the base of the TAG active mound, where adult shrimps were scattered over large areas (Table 1, Fig. 1E, Fig. S2A-C Appendix B). At Snake Pit, 6 samples were collected in dense shrimp aggregations on the walls of active chimneys of the Beehive site (Table 1, Fig. 1C, Fig. S1A-E Appendix B). Distance between each sample within each vent field varied from one meter to tens of meters (Fig. 1B-C).

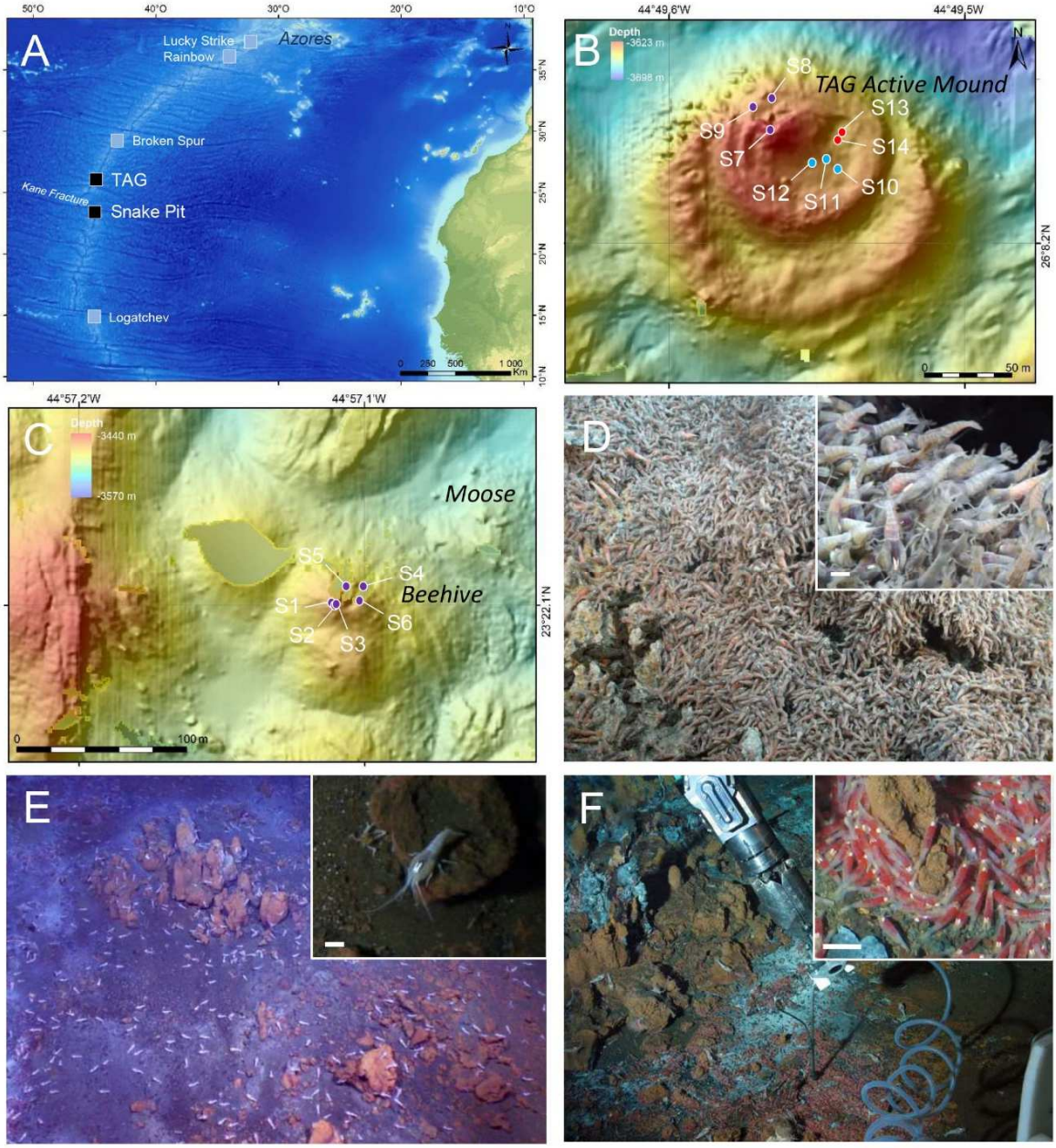

Figure 1. Sampled vent fields and shrimp assemblages. A) North Atlantic map (Amante, C. and B.W. Eakins, 2009. doi:10.7289/V5C8276M) with the main active vent fields known on the Mid Atlantic Ridge and our study sites denoted with black squares ; B) Location of the samples collected on TAG active mound ; C) Location of the samples collected on the Beehive edifice of Snake Pit field ; B-C : colours denote assemblage types : dense aggregations in purple, scattered assemblages in blue, nurseries in red ; D) Dense *R. exoculata* aggregation ; E) Scattered *R. exoculata* assemblage ; F) Nursery of small juveniles ; D-F : Pictures from TAG vent field, scale bars in close-up views : 1 cm.

137 Shrimps were collected with the suction sampler of the Remotely Operated Vehicle (ROV)
138 Victor6000. In dense aggregations and nurseries, the tip of the sampler was placed in contact
139 with individuals and maintained immobile during suction to avoid disturbance as much as
140 possible. The suction was activated for a few seconds in order to collect individuals from a small
141 area (less than 0.05 m^2). Scattered shrimps were sampled by sweeping the tip of the suction
142 sampler over seafloor areas of a few m^2. This larger sampling area was necessary to gather a
143 sufficient number of individuals. In addition, 37 individuals caught with a baited (with fresh fish
144 meat) shrimp-trap deployed for 5 days on inactive substratum at TAG (S12) were included in the
145 analyses. A total of 3 445 specimens were examined (Table 1, Hernández-Ávila et al. 2021).

146 **Table 1.** Shrimp sample details, including temperature ranges measured within centimeters from
147 the assemblage sampling point when available. ND: no data available.

Vent Field	Dive	Sample	Sample size (ind.)	Juveniles for genetics	Assemblage type	Depth (m)	T (°C)
SP	PI01-564-Aspi3	S1	143		dense	3463	3.5-22
SP	PI01-564-Aspi4	S2	390		dense	3463	3.5-22
SP	PI01-564-Aspi5	S3	808		dense	3463	3.5-22
SP	PI05-568-Aspi1	S4	391		dense	3465	10-21
SP	PI05-568-Aspi4	S5	110		dense	3468	4-18
SP	PI05-568-Aspi6	S6	364	1	dense	3472	ND
TAG	PI08-571-Aspi2	S7	600	4	dense	3626	8-14
TAG	PI10-573-Aspi1	S8	207		dense	3624	6-33
TAG	PI10-573-Aspi2	S9	161		dense	3627	3-30
TAG	PI10-573-Aspi5	S10	18		scattered	3635	2.4-2.8
TAG	PI10-573-Aspi6	S11	38		scattered	3635	2.4-2.8
TAG	PI12-575-Nasse 2	S12	37		scattered	3634	2.4-2.8
TAG	PI08-571-Aspi1	S13	77	36	nursery	3637	2.8-5.3
TAG	PI12-575-Aspi2	S14	101	36	nursery	3637	2.8-5.3

148

149 Temperature measurements were conducted along with shrimp collections. Records were
150 obtained either from discrete measurements with the submersible temperature probe prior to

151 sampling, or from time-series measurements with autonomous temperature probes (WHOI-MISO
152 low temp-ONSET®) deployed within the shrimp aggregation for a few days prior to sampling.

153 **2.2. Identification and measurements**

154 Specimens were identified and classified as juveniles, subadults or adults, in accordance
155 with Komai and Segonzac (2008), and using the size of the onset of sexual determination (OSD,
156 Suppl. data Appendix A) to sort subadults from small adult females which are morphologically
157 nearly identical. Individuals resembling adult females with sizes < OSD were considered as
158 subadults. The identification of the smaller juveniles from nurseries was further assessed by DNA
159 analyses because their morphology did not fit completely the description of early juvenile stages
160 (stage A) of *R. exoculata* available at the time of this study (Komai and Segonzac, 2008). Thirty-
161 six juveniles from each nursery and 5 juveniles from dense aggregations were used for molecular
162 identifications (Table 1, Table S1 Appendix B).

163 Sex was identified in adults by the occurrence of the “appendix masculina" on the second
164 pleopod in males, and the shape of the endopod of the first pleopod (Komai and Segonzac, 2008).
165 Since these sexual characters appear during the transition from subadult to adult stage, sex of
166 juvenile and subadult specimens could not be determined. Brooding females were characterized
167 by the presence of embryos held between their pleopods under the abdomen, and by
168 modifications of their pleopods (addition of setae to maintain the brood). Hatched females
169 (females just after larval release but prior to molt) were identified by their modified pleopods.
170 Brooding and hatched females were referred to collectively as ovigerous females (following Nye
171 et al. 2013). We also defined a size of effective sexual maturity (ESM) representing the minimal
172 size at which females spawn (Suppl. data Appendix A). Females larger than ESM were called
173 sexually mature females.

Carapace length (CL) was measured from the posterior margin of the ocular shield to the mid-posterior margin of the carapace in adults and subadults (Fig. 2a), with a precision of 0.1 mm. In juveniles, CL was measured from the anterior tip of the rostrum to the posterior margin of the carapace (Fig. 2b). Morphological changes between juvenile and adult stages (rostrum reduction and development of the ocular shield) may introduce a bias in our measurements but this was small compared to the total length of the carapace, and had little impact on size frequency distributions and size comparisons.

Embryos were removed from the abdomen of brooding females, counted and staged. We classified embryonic developmental stages into 3 categories, similar to those defined by Nye et al. (2013) for *R. hybisae*. Early stage embryos encompass freshly laid fertilized eggs without cellular division, and dividing eggs until the blastula stage (Fig. 2C-D). Mid stage starts with gastrulation when a clear region differentiates at one pole of the embryo and extends to the end of the naupliar development (Fig. 2E-F). Late stage includes post-naupliar development, when eye pigmentation becomes visible, abdomen appears clearly separated from the rest of the body with yolk in the cephalothorax, and appendages are fully lengthened and appear curled around the cephalothorax (Fig. 2G). For each brood, ten embryos were randomly selected and both their maximum and minimum diameters were measured at a precision of 0.03 mm under a stereomicroscope with a graduated ocular. The volume of embryos was estimated according to Oh and Hartnoll (2004), considering a spheroid volume as $v= (4/3) \pi r_1 r_2^2$, where r_1 and r_2 are half of the maximum and minimum axis, respectively. This estimation has a precision of 1.6×10^{-5} mm^3.

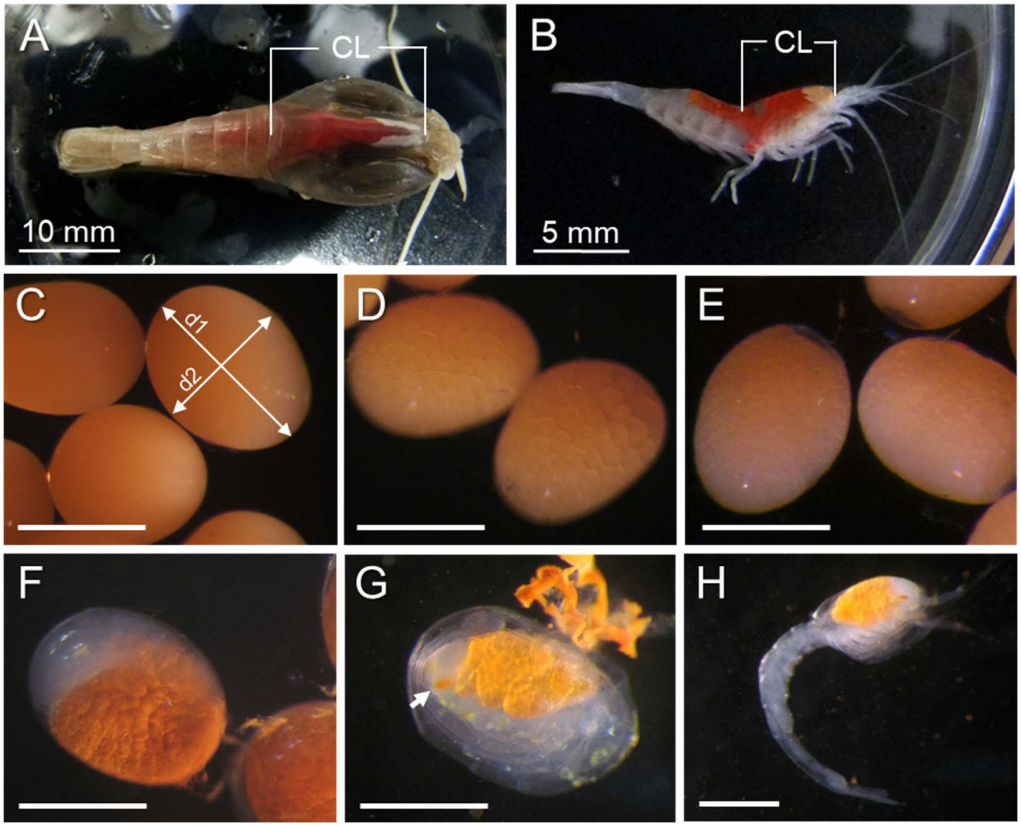

Figure 2. Size measurements of different life stages of *Rimicaris exoculata*. A) Adults and subadults. B) Juveniles. C-H) Embryos and hatched larvae. Early developmental stage: C) Fertilized egg (with position of measurements for maximum (d1) and minimum (d2) diameters), D) Blastula stage; Mid developmental stage: E) Early gastrulation, F) Nauplius stage; Late developmental stage: G) Pre-hatch embryo (arrow indicates eye spot). H) Hatching Zoea larva. CL: carapace length. Scale bars C-H: 500 µm.

2.3. Genetic identifications

DNA was extracted from muscle tissues of juveniles using the CTAB method (Doyle 1990). A section of the cytochrome oxidase I gene (COI) was amplified in a 50 µL solution of 1X reaction buffer, 2 mM $MgCl_2$, 0.25 mM dNTP, 1.2 units of Taq polymerase and 0.6 mM of each primer (LCOI1490 and HCOI2198, Folmer et al. 1994). Amplifications were performed as follows: initial denaturation (5 min at 95°C), 40 cycles including denaturation (1 min at 94°C), annealing (1 min at 52 °C) and extension (2 min at 72 °C), followed by a final extension of 7 min at 72°C. All PCR

amplifications were conducted on a GeneAmp PCR system 9700 (Applied Biosystems). PCR products were purified and sequenced by Macrogen, Inc. (Netherlands) using the amplification primers. Accession number of each sequence is provided in Table S1 (Appendix B). We aligned our sequences using MUSCLE (Edgar, 2004), along with a set of alvinocaridid and other shrimp sequences. A neighbor-joining tree was constructed using Geneious R8 software (Kearse et al. 2012) using a HKY evolutionary model of nucleotide substitution. Robustness of the inferred tree was evaluated using bootstrap method with 1000 replicates.

2.4. Data analysis

For each sample, juvenile ratio, subadult ratio and sex ratio (F:M) were estimated. Deviation from a sex ratio of 1:1 was tested with a χ^2 test, using Yates correction in samples with few specimens ($n < 30$). In order to assess the variability in ratios between samples of a same type of assemblage at each vent field, we performed a heterogeneity χ^2 test (Zar, 2010). Variations in the proportions of sexually mature females or ovigerous females between vent fields were tested using χ^2 test.

Size class structures were analyzed for each sample, estimating kurtosis and skewness for size class aggregation and deviation from the mean, respectively (Zar, 2010). Although histograms were elaborated denoting juveniles, subadults, males and females, size structure comparisons were performed including all specimens. Normality tests were performed for each sample using the Shapiro-Wilk test (Zar, 2010). Discrete size cohorts in samples from dense aggregations were identified using the statistical package mixdist (MacDonald, 2003) running in R™. The goodness of fit of the identified size cohorts was verified using χ^2 test. Identification of cohorts in other types of assemblages were not performed due to insufficient sample size.

For samples from dense aggregations, differences in body sizes associated with sex and vent fields were tested using multifactorial analysis of variance (ANOVA), after $\log_{10}$

transformation. For this analysis, samples were nested at the factor vent field, representing the variation in body size between samples collected randomly within dense aggregations within the same vent field. Similarly, an ANOVA test was performed in order to examine differences in male body sizes between assemblage types (dense vs scattered) at the TAG vent field. In this case, samples were nested at the factor assemblage type. Data normality and homoscedasticity were tested using χ^2 for frequency distribution and Levane test respectively (Underwood, 1997, McGuinness, 2002).

The difference in size-specific fecundity between vent fields was tested using a t-test analysis. Variations in embryo size associated with parental female, embryo stage and vent fields were analyzed with a multifactorial ANOVA test. For this analysis the factor parental female was considered as nested to the combination of vent field and embryo stage.

3. Results

3.1. *Rimicaris* shrimp populations at TAG and Snake Pit in January 2014

Among the 3445 individuals collected in our samples, we determined developmental stage and sex for 3388 individuals and measured 3379 individuals (missing data are due to body damages preventing accurate measurements or sex/stage determination). The global dataset included 1925 females (56.8%), 292 males (8.6%), 882 subadults (26.1%) and 289 juveniles (8.5%). Global sex-ratio clearly deviated from 1:1 (χ^2, df= 1, $p< 0.01$). Of the 1925 females, 136 (7.1%) were either brooding eggs (125), or had recently hatched larvae (11).

Smaller specimens were early juveniles (CL = 4.4 mm), whereas the largest one was a female with 24.4 mm CL (but this was an outlier since the next largest females were ~20.6 mm CL). Size-range of the juveniles was 4.4 to 10.3 mm, and overlapped the subadult size range (7-9.9 mm CL) (Table S2 Appendix B). The onset of sexual differentiation (OSD) was estimated at

10 mm CL (Suppl. data Appendix A), which is consistent with the size of the smallest adult male found in our samples (CL = 9.9 mm). Although the size of some juveniles exceeded the OSD size, they were morphologically distinct from subadults: their rostrum was not completely reduced, and their carapace not fully inflated.

Overall, size ranges of males and females were similar with respective CL ranges = 9.9-19.1 mm and 10-24.4 mm (Table S2 Appendix B). However, the average size of males was greater than the average size of females, with 15.1 mm CL and 12.5 mm CL respectively (t-test= 20.71, $p < 0.001$). Most ovigerous females exhibited large sizes, with CL ranging from 12 mm to 20.6 mm (average size: 16.5 mm CL). We estimated the size at effective sexual maturity (ESM) at 15.1 mm CL for females (Suppl. data Appendix A).

3.2. Variation in population structure across assemblage types and vent fields

3.2.1. Habitat characteristics of shrimp assemblages

In dense aggregations, the substratum was completely covered by shrimps, sometimes with multiple layers of individuals. Vent fluids were visibly bathing these assemblages and we recorded steep temporal variations in temperature with maxima varying from 14 to 33°C (Table 1). On inactive sulfide substratum at the periphery of dense aggregations, we visually estimated shrimp densities around 10 individuals.m^{-2}. These scattered individuals were collected only at TAG, although similar assemblages were also observed at Snake Pit. In this habitat, no fluid exit was visible and temperature was low and stable, with a maximum of 2.8°C (Table 1), whereas ambient seawater temperature was 2.6°C. At TAG, aggregations of very small individuals characterized by their bright red color were sampled around diffusions of translucent fluids exiting from very small chimneys or cracks. Temperatures in these nurseries varied from 2.8°C to 5.3°C (Table 1). The 3 types of assemblages with visually distinct shrimp densities, sizes and behavior were thus also characterized by different temperature regimes reflecting the local exposure to vent fluids.

3.2.2. Variations in population structure between assemblage types (TAG)

At TAG, we observed striking differences in terms of population structure, size-frequency distribution, and reproductive features between the three types of assemblages. In dense aggregations, with 71% of females and 8.5% of males, sex-ratio was clearly biased towards females (F:M=8.4:1). Although sex ratios were significantly different between dense aggregation samples from TAG ($\chi^2 het$= 50.05, df= 2, p< 0.001, Table 2), all of them were significantly female biased (χ^2, df= 1, p< 0.02 in all cases, Table 2). In contrast, in scattered assemblages, 90.3% of the individuals were males, while females represented only 6.5% of the shrimps collected. Sex ratio was significantly male-biased overall (1:14) and in each sample (χ^2, df= 1, p≤ 0.002 in all cases, Table 2). Subadults represented 17.5% of the individuals on average in dense aggregations (Table 2), with significant variation between samples (from 3% to 23.2% of the individuals in each sample, $\chi^2 het$= 16.4, df= 2, p< 0.001). Subadults were rare in scattered assemblages with only two individuals collected overall.

Ovigerous females were almost exclusively observed in dense aggregations at TAG (only one hatched female observed among scattered assemblages and none in nurseries), representing 11.7 % of the females on average, with strong variations between samples (from 8.4% to 25.6%). These variations reflect both variations in the proportion of sexually mature females among all females (22.4% on average, with variations between samples: 13.3% to 64.9%), and, to a lesser extent, variations in the proportion of ovigerous females among sexually mature females (36.8 % on average, with variations between samples: 29.8% to 43.6%).

Juveniles represented less than 3% of all shrimps in dense aggregations (Table 2, no significant heterogeneity between samples: $\chi^2 het$= 3.64, df= 2, p= 0.602), and were rare in samples from scattered assemblages with only one early stage juvenile collected. In contrast, nursery samples were exclusively composed of early stage juveniles. Although they were not

collected, a few large adult individuals (both *R. exoculata* and *R. chacei*) were observed crawling around these nurseries (Fig. 1F, Fig. S2D-E Appendix B).

Table 2. *R. exoculata* specimens and sex ratios in the different samples. J: juveniles, <OSD (onset of sexual differentiation): subadults, F: females (non-ovigerous); OF: ovigerous females; M: males.

Dense aggregations										
Vent field	Sample	J	<OSD	F	OF	M	n	F : M	χ^2	p
Snake Pit	S01	1	8	109	1	20	139	5.5:1	62.308	<0.001
Snake Pit	S02	14	175	181	2	9	381	20.3:1	157.688	<0.001
Snake Pit	S03	6	177	522	29	53	787	10.6:1	410.603	<0.001
Snake Pit	S04	16	188	174	0	6	384	29:1	156.8	<0.001
Snake Pit	S05	26	22	39	1	20	108	2:1	6.667	0.01
Snake Pit	S06	21	143	158	22	19	363	9.5:1	130.256	<0.001
Total								9.8:1	904.264	<0.001
							Heterogeneity		20.056	0.001
TAG	S07	19	138	380	35	23	595	18:1	350.831	<0.001
TAG	S08	1	6	163	25	7	202	26.7:1	168.005	<0.001
TAG	S09	6	23	58	20	51	158	1.5:1	5.651	0.017
Total								8.5:1	472.441	<0.001
							Heterogeneity		50.046	<0.001
Scattered assemblages										
TAG	S10	1	0	2	0	15	18	1:7.5	9.941	0.002
TAG	S11	0	2	2	1	33	38	1:16	25	<0.001
TAG	S12	0	0	1	0	36	37	1:35	33.108	<0.001
Total								1:16	67.6	<0.001
							Heterogeneity		0.449	0.993
Nurseries										
TAG	S13	77	0	0	0	0	77			
TAG	S14	101	0	0	0	0	101			

3.2.3. Variation in population structure between vent fields (dense aggregations only)

313 Samples in dense aggregations from Snake Pit exhibited similar population structure to
314 those from TAG, with a strong dominance of females. Females, males, subadults and juveniles
315 represented respectively 57.2%, 5.9%, 33 % and 3.9% of the overall population. Sex-ratio was
316 female-biased (9.8:1 overall) and similar to the ratio observed in TAG dense aggregations. Like
317 in TAG, sex-ratio varied significantly among dense aggregation samples at Snake Pit ($\chi^2 het$=
318 20.06, df= 5, p= 0.001, Table 2), but all were significantly female-biased (χ^2, df= 1, p≤ 0.01 in all
319 cases).

320 Overall, subadults were more abundant in Snake Pit samples than in TAG samples,
321 representing almost a third of the population. However, their proportion varied strongly between
322 samples (from 5.8% to 45.9% of the individuals, $\chi^2 het$= 164.9, df= 5, p< 0.001). Like in TAG dense
323 aggregations, the proportion of juveniles in Snake Pit samples was generally low, except in one
324 sample where they reached 24.1% of the individuals, resulting in significant heterogeneity
325 between Snake Pit samples ($\chi^2 het$= 89.32, df= 5, p< 0.001).

326 Although the proportion of ovigerous females among sexually mature females was similar
327 between vent fields (36.6 % on average at Snake Pit, χ^2= 0.003, p= 0.956), the proportion of
328 sexually mature females among all females was significantly lower in Snake Pit (11.7 %) than in
329 TAG (22.4 %) dense aggregation samples (χ^2= 34.24, p< 0.001), resulting in lower proportion of
330 ovigerous females overall (4.4% of all females).

331 *3.2.4. Variations in size frequency distributions among assemblage types and vent fields*

332 Overall, reflecting the differences in sex and stage distributions between types of
333 assemblages, size distributions also differed. While nurseries hosted very small shrimps, almost
334 none were found in other assemblage types. Mostly large individuals inhabited scattered
335 assemblages. In dense aggregations, shrimp sizes varied over a wide range, overlapping slightly
336 both size ranges of shrimps in nurseries and scattered assemblages (Fig. 3, Fig. S3 Appendix B).

337 Size frequency distributions varied between samples and assemblage types, both in terms
338 of kurtosis and skewness (Fig. 3). General trends in dense aggregation size frequency
339 distributions include bias towards small sizes (skewness= 0.945) and slightly leptokurtic
340 distribution (kurtosis= 0.423). In some samples, the distribution was clearly non-unimodal. In
341 others, deviation in skewness and kurtosis suggested a mixture of cohorts. Based on a size cohort
342 analysis of each sample, we visually identified 5 different cohorts overall in dense aggregations
343 (Table 3). The first comprised juveniles and smaller subadults, the second subadults and small
344 adults, and the last 3 cohorts consisted only of adults, with sexually mature females in the last
345 two. In both vent fields, the cohorts corresponding to juveniles, subadults and small adults
346 represented an important proportion of the population of dense aggregations. In individual
347 samples, cohort number varied between 2 to 4 (Table 3, Fig. S4 Appendix B).

348

349

350

351

352

353

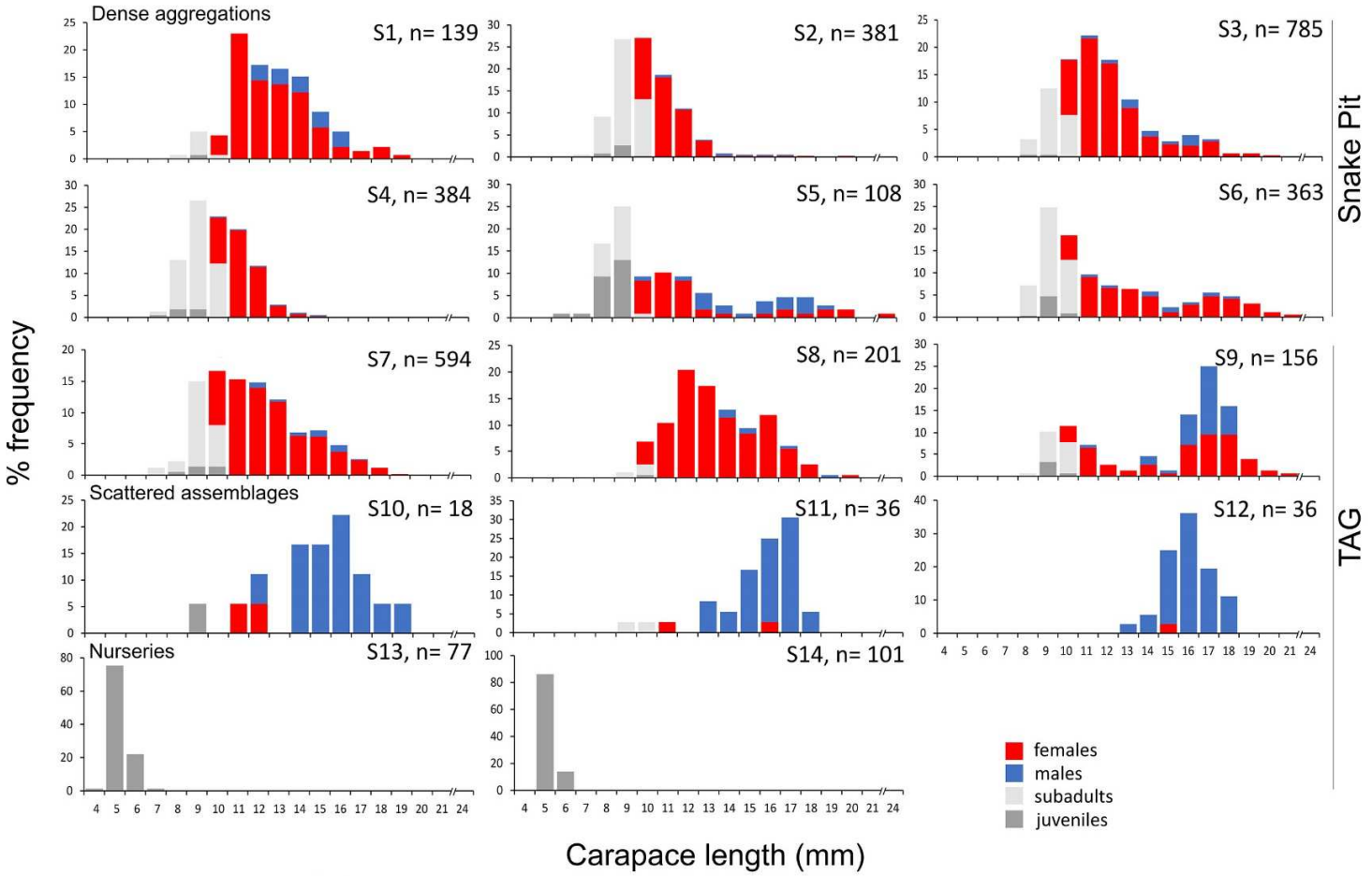

354

355 **Figure 3.** Size class structure of *R. exoculata* from each sample collected in different assemblages at Snake Pit and TAG vent fields.

Table 3. Identified cohorts in dense shrimp aggregations at the Snake Pit and TAG vent fields. Mean and standard deviations are shown for each sample, proportion of each cohort are in brackets. Correspondence of cohorts between samples was visually defined but not statistically tested. χ^2 denote the deviation of the sample from the cohort estimation. ns: non-significant.

Cohort:	1	2	3	4	5	χ2
Snake Pit						
S1		11.45±1.75 (0.59)	13.24±2.03 (0.41)			12.93ns
S2	8.86±0.87 (0.61)	10.78±1.06 (0.37)		16.14±1.58 (0.02)		3.058ns
S3	9.14±0.89 (0.33)	11.25±1.09 (0.54)		15.49±1.50 (0.13)		11.16ns
S4	8.45±0.77 (0.50)	10.47±0.96 (0.48)	12.92±1.18 (0.02)			1.995ns
S5	8.30±0.87 (0.52)	11.40±1.19 (0.28)			17.28±1.80 (0.20)	15.32ns
S6	8.70±0.70 (0.47)	10.44±0.84 (0.17)	12.81±1.03 (0.17)		17.11±1.38 (0.19)	3.247ns
TAG						
S7	9.83±1.40 (0.59)		13.38±1.90 (0.41)			25.11*
S8		10.12±0.83 (0.15)	12.17±1.00 (0.51)	15.39±1.27 (0.34)		3.556ns
S9	8.98±0.53 (0.21)	10.50±0.62 (0.11)	13.37±0.79 (0.06)		16.73±0.99 (0.62)	8.230ns

*Despite the deviation of the size structure from the cohort model (p= 0.0485), it was the closest model to the observed data

Male and female body sizes in dense aggregations were significantly different between samples at each vent field, indicating heterogeneity in sizes within this type of assemblage (ANOVA, p< 0.001, Table S3 Appendix B). Body sizes also varied significantly with sex (ANOVA, p< 0.001, Table S3 Appendix B), males being larger than females at each vent field (Table S2 Appendix B). Size distribution of ovigerous females clearly departed from the rest of the females, with sizes similar to the male average size in TAG and even larger than the male average size in Snake Pit. Although males and females tended to be smaller in Snake Pit than in TAG dense aggregations, size differences were not significant between the two vent fields for each sex (ANOVA, p= 0.083, Table S3 Appendix B). In contrast, ovigerous females were slightly larger in

371 Snake Pit than in TAG dense aggregations, but this variation between the two vent fields was not
372 statistically significant (ANOVA F= 1.649, p= 0.246, df_2= 6).

373 Size frequency distributions in scattered assemblages were leptokurtic (kurtosis 0.12 to
374 1.99) and biased towards larger sizes (skewness -0.45 to -1.52). Males exhibited no difference in
375 body sizes between dense aggregations and scattered assemblages, although significant
376 difference was detected between samples of a given type of assemblage (ANOVA, p< 0.001,
377 Table S4 Appendix B). Females also exhibited similar size ranges between assemblage types,
378 although the low number of females collected in scattered assemblages prevented statistical
379 comparisons.

380 *3.2.5. Juvenile distribution in dense aggregations and nurseries*

381 Juvenile sizes in dense aggregations were similar between vent fields, only showing
382 differences between samples (ANOVA F_{vents}= 5.2001, p= 0.057, df_2= 7, $F_{samples}$= 2.643, p= 0.015,
383 df_1= 7, df_2= 101). However, juveniles from nurseries were much smaller (ANOVA F_{vents}= 804.91,
384 p< 0.001, df_2= 3, $F_{samples}$= 1.580, p= 0.195, df_1= 3, df_2= 199) and formed a distinct cohort from that
385 of dense aggregations. Based on morphological features described in Komai and Segonzac
386 (2008), we suspected that juveniles from nurseries were possibly a mixture of *R. exoculata* and
387 *R. chacei*. COI sequences from juveniles with various morphological features in nurseries were
388 all consistent with *R. chacei* affiliation, whereas sequences from juveniles in dense aggregations
389 were consistent with *R. exoculata* affiliation (Fig. S5 Appendix B).

390 **3.3. Reproductive features**

391 *3.3.1. Fecundity*

392 Of the 125 brooding females collected, 36 had obviously lost part of their broods, not
393 because of hatching (embryos were clearly not yet fully developed), but rather due to either

394 abortion or more probably loss during sampling. These were not included in our fecundity
395 analyses.

396 Fecundities varied from 304 eggs in a female from TAG with 16.2 mm CL, to 1879 eggs
397 in a female from Snake Pit with 19.8 mm CL. The largest brooding females were observed at
398 Snake Pit (with 1704 eggs and 20.5 mm CL for the largest), while the smallest brooding females
399 were from TAG (with 500 and 532 eggs for the two smallest -12 mm CL- individuals). The overall
400 average fecundity was 833 eggs, and was higher among Snake Pit brooding females (1045 eggs,
401 with an average CL of 17.4 mm) than among TAG ones (616 eggs, with an average CL of 15.9
402 mm). As expected, a positive correlation was observed between carapace length of the females
403 and fecundity (Pearson correlation, R= 0.682, *t-test*= 8.71, p< 0.001) (Fig. 4). We consider that
404 more data are necessary to estimate accurate linear regression models of fecundity and compare
405 differences between populations of the two vent fields or with other alvinocaridid shrimps.

406 Overall size-specific fecundity ranged from 19 to 95 embryos.mm^{-1} CL. The size-specific
407 fecundity of females did not change with the developmental stage of the brood (Early vs Mid
408 stage, t-test= 0.98, p= 0.164, df=57; Mid vs Late stage, t-test= 0.17, p= 0.432, df=57), but was
409 significantly lower in females from TAG (39 ± 10 embryos.mm^{-1} CL) than in females from Snake
410 Pit (59 ± 13 embryos.mm^{-1} CL) (t-test=8.16, p<0.001, df=87). In addition, more females with
411 damaged broods were observed at TAG.

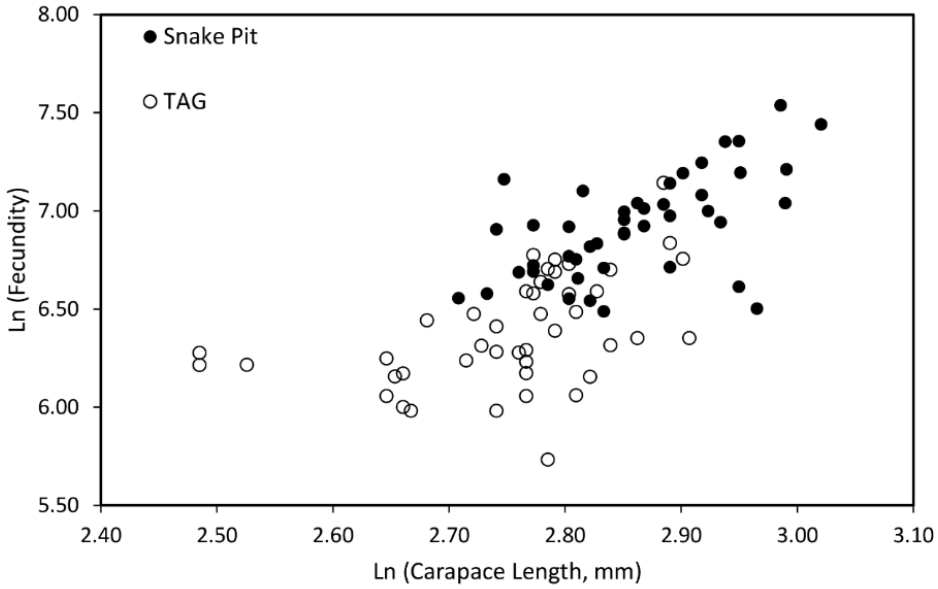

412

413 **Figure 4.** Relationship between fecundity and size in *R. exoculata* from TAG and Snake Pit vent
414 fields.

415 *3.3.2. Reproductive synchrony*

416 Within each individual brood examined, all eggs were at the same developmental stage
417 (early, mid or late), except for occasional dead embryos or non-fertilized eggs. However, embryos
418 at all developmental stages were observed in females from each vent fields, showing a lack of
419 synchrony between females. Overall, the distribution of brood stages was different between vent
420 fields (χ^2= 7.097 p=0.014), with variability between samples of a given vent field (Fig. S6 Appendix
421 B). At each vent field, a third of the females carried early stage broods, however at Snake Pit late-
422 stage brooding and hatched females were slightly more frequent (37%) than at TAG (19%). At
423 TAG, most of the brooding females were at the mid stage (51.9%) (Fig. 5A).

424

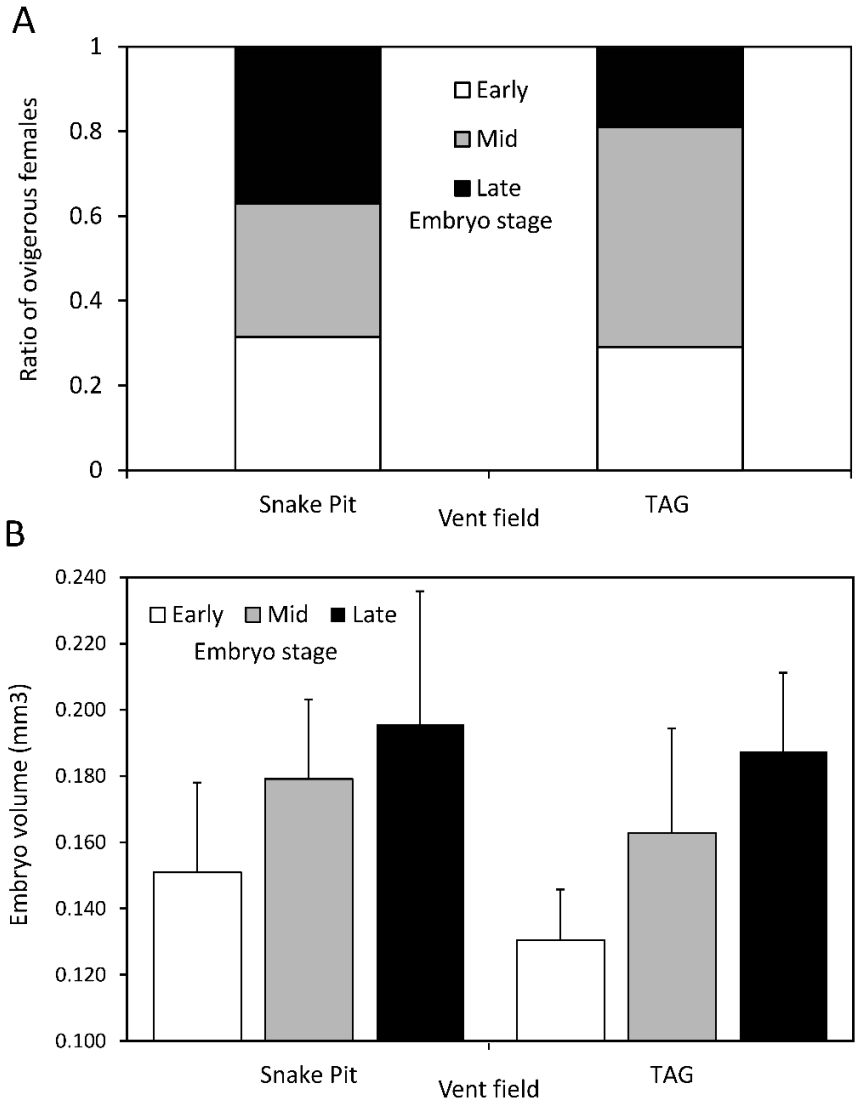

425

426 **Figure 5.** Characteristics of *R. exoculata* broods at TAG and Snake Pit vent fields. A. Proportion
427 of broods with eggs at each developmental stage (including hatched females as having late
428 broods). B. Sizes of individual embryos at different developmental stages.

429 *3.3.3. Egg sizes and development*

430 The volume of the eggs within the brood of each female showed significant heterogeneity
431 due to inter-individual variations, developmental stage of the broods, and vent fields (Table S5
432 Appendix B). Despite individual variations, a clear trend of egg volume increase with
433 developmental stages was observed at each vent field (Fig. 5B). The ratio between the minimum

434 and maximum diameters of embryos decreased along their development, with minimum diameter
435 being on average 0.87 of the maximum diameter in early stage, and 0.76 of the maximum
436 diameter in the late stage. Eggs thus become more elongated at the end of embryonic
437 development, which may reflect an increase of the embryo polar axis, the distribution of the
438 structures inside the envelope and water uptake.

439 At each stage, embryos in TAG broods were smaller than in Snake Pit broods (Fig. 5B).
440 The volume of early stage embryos was 0.151 ± 0.027 mm^3 at Snake Pit, and 0.131 ± 0.015 mm^3
441 at TAG (*t-test*= 8.386, p< 0.001, df=242). At mid-stage, the volume of embryos increased to 0.179
442 ± 0.024 mm^3 at Snake Pit and 0.163 ± 0.032 mm^3 at TAG (*t-test*= 3.719, p< 0.001, df= 116). In
443 the late stage, the volume of embryos reached 0.196 ± 0.040 mm^3 at Snake Pit and 0.187 ± 0.024
444 mm^3 at TAG (*t-test*= 2.458, p= 0.007, df= 238).

445 **4. Discussion**

446 Populations of *Rimicaris exoculata* sampled in January-February 2014 at TAG and Snake
447 Pit vent fields revealed strikingly biased sex ratios, reflecting abrupt changes in population
448 structure among different shrimp assemblages. Dense aggregations next to high temperature
449 fluid exits consisted mainly of females and immature individuals, whereas shrimps observed
450 scattered in the cold and stable periphery of active vents were almost only adult males. At TAG,
451 assemblages of very small juveniles around low temperature diffusions were *Rimicaris chacei*
452 nurseries, whereas *R. exoculata* juveniles were found in the denser aggregations. Ovigerous
453 females were observed in larger proportion than ever reported so far for this species, representing
454 about a third of the sexually mature females in dense aggregations. Overall, these patterns were
455 consistent across both vent fields, although a high degree of heterogeneity in population structure
456 was observed at small spatial scale, across dense aggregations. Ovigerous females were more
457 abundant at TAG, reflecting a higher proportion of sexually mature females. However, lower

458 fecundities and smaller eggs were observed in ovigerous females from TAG, suggesting a lower
459 individual reproductive effort.

460 **4.1. Spatial variability in *Rimicaris* population structure**

461 *4.1.1. Sex segregation in different types of assemblages*

462 At TAG, we showed that dense aggregations of *R. exoculata* shrimps on active chimneys
463 and scattered individuals occurring in peripheral areas with no visible fluid exits have very different
464 population structures. Although they were reported in previous studies (Copley et al. 1997, 1999,
465 Segonzac et al. 1993), scattered shrimps were not included in demographic studies so far,
466 probably because they have been considered as remains of the main populations. Our
467 observations show that these scattered shrimps represent a truly specific assemblage consisting
468 mainly of large males, whereas females and immature individuals which constitute the bulk of the
469 population in dense aggregations are rarely observed at the periphery. At Snake Pit, dense
470 aggregations were also dominated by immature individuals and females, and scattered shrimps
471 were observed in inactive peripheries nearby the main active edifices. Although these shrimps
472 were not collected at Snake Pit, they were visually mirroring scattered assemblages from TAG
473 and comprised mostly large adults. We thus expect these shrimps, as well as scattered individuals
474 reported from other vent fields (Segonzac et al. 1993, Copley et al. 1997, 1999) to be also mainly
475 males. Complex population distributions with local variations in densities and structure are likely
476 general features of *R. exoculata* populations along the MAR.

477 Differentially distributed males and females with locally unbalanced sex-ratios have been
478 reported in several crustaceans from deep-sea vents and seeps. For instance, populations of
479 *Rimicaris hybisae* at the Cayman Trough vents have a sex ratio in favor of females close to the
480 fluid emissions, while more dispersed populations are dominated by males at their peripheries,
481 with some degree of local variability (Nye et al. 2013). At hydrothermal vents of the East Scotia

Ridge, the chirostylid crab *Kiwa tyleri* exhibits similar -but inverse- patterns: areas close to vent fluids emission are occupied by dense male-dominated aggregations, whereas females are more numerous at the periphery (Marsh et al. 2015). In brine pools of the Gulf of Mexico, *Alvinocaris stactophila* shows overall female-biased sex ratio with most males locating in areas exposed to sulphidic and hypoxic conditions, whereas large reproductive females occupy less exposed areas (Copley and Young 2006). Biased sex ratios, with small scale variability associated to environmental conditions thus appear to be a common feature of populations of vent and seep decapods, although the distribution of each sex within the fluid exposure gradient depends on species.

4.1.2. Patchiness in dense aggregations

At a smaller scale, within dense *R. exoculata* aggregations of each vent field, we also observed heterogeneity in population structures, with significant variations in the proportions of the different life stages between our samples. Brooding females were found in significant numbers in 5 out of 9 samples whereas they were almost absent from the 4 remaining, suggesting they have a patchy distribution across those dense aggregations. Similarly, juveniles occurred in significant proportion in only one sample from Snake Pit, again reflecting a patchy distribution of this life stage. Patchiness within dense shrimp aggregations was already suggested in populations of Logatchev and other vent fields because gatherings of juveniles among adults are visually conspicuous (Gebruk et al, 2010, Shank et al, 1998). Our results confirm the spatial heterogeneity in the distributions of the different life stages across dense aggregations, with local segregation patterns. Similar spatial segregation between benthic life stages at vents were reported in *Bathymodiolus* mussels (Husson et al. 2017) and in chyrostylid crabs (Marsh et al. 2015). These patterns have been related to local habitat conditions, life stage physiological requirements or tolerances, as well as resource use (Husson et al. 2017). In *R. exoculata* dense

aggregations, additional observations are necessary to refine small-scale population structures and their links with local environmental gradients and resource availability.

4.1.3. Distinct nurseries for R. exoculata and R. chacei

Rimicaris juveniles were reported from dense aggregations on vent chimney walls and isolated patches at the base of edifices, in Logatchev (Gebruk et al. 2000), and other vent fields along the nMAR (Shank et al. 1998). They were identified as *R. exoculata* (Shank et al. 1998) or mixtures of both *R. exoculata* and *R. chacei* co-occuring in the same patches (Komai and Segonzac 2008). Our molecular data demonstrated that small juveniles in isolated low temperature nurseries were all *R. chacei*. In contrast, juveniles in dense aggregations belonged to *R. exoculata*, suggesting that juveniles of both species segregate in distinct habitats, with different temperature conditions. Aggregations of small juveniles of *R. chacei* were also observed around fluid diffusions at the periphery of TAG and Snake Pit vent fields during following cruises in 2017 and 2018 (Methou et al. 2020). A more systematic examination of morphological characters along with molecular characterization led to a redefinition of the juvenile stages of each *Rimicaris* species (Methou et al. 2020). In our 2014 samples, we identified all stages defined by Methou et al. (2020), *R. chacei* juveniles all being in isolated low temperature nurseries, while *R. exoculata* juveniles at all stages occurred in dense aggregations.

The size difference between *R. chacei* and *R. exoculata* juveniles in our samples suggests that we may miss earlier benthic stages for the latter, assuming a similar settlement size between the two species. However, a single *R. exoculata* pelagic post-larva was caught in nets towed within the axial valley of the MAR 200-1000 m above the Broken Spur vent field in August and September 1995, probably as it was approaching its recruitment place. It had a size similar to those of our benthic *R. exoculata* juveniles (28 mm total length) in dense aggregations, whereas post-larvae of *R. chacei* caught at the same time were smaller (13-23 mm) (Herring and Dixon

530 1998) and similar to our *R. chacei* juveniles from low temperature nurseries. This implies a larger
531 settlement size in *R. exoculata*, and undermines the possibility that we missed an earlier benthic
532 stage that would settle elsewhere or at another period. Isotopic analyses conducted on *R. chacei*
533 juveniles from isolated nurseries and on *R. exoculata* juveniles within dense aggregations at our
534 study sites also support a higher settlement size for the latter (Methou et al. 2020). Smallest
535 juveniles of each species harbor an isotopic signature reflecting nutrition on material of
536 photosynthetic rather than chemosynthetic origin, which suggests that both recently left the
537 pelagic realm to start their benthic life, settling at different sizes. Juveniles of each species thus
538 not only differ in their settlement habitats but also in their settlement size, which probably affects
539 their post-settlement life history.

540 **4.2. Reproductive development in *R. exoculata***

541 *4.2.1. Temporal variability in spawning*

542 Despite three decades of sampling at MAR hydrothermal vents, reports of *R. exoculata*
543 brooding females were extremely rare (Gebruk et al. 1997, Ramirez-Llodra et al. 2000) except in
544 March 2007 on the Logatchev vent field (Gebruck et al. 2010), but very few individuals were
545 collected at that time (Komai and Segonzac 2008, Guri et al. 2012). In January-February 2014,
546 7.1% of the females collected in our samples were brooding eggs or had just released their larvae.
547 This apparently low proportion essentially reflects the high proportion of small females below the
548 size of sexual maturity. Indeed, a third of the sexually mature females were ovigerous at each
549 vent field. In addition, many of the two remaining thirds exhibited bright pink well developed
550 gonads dorsally, suggesting that these females were ready to spawn (FP personal observation
551 on our samples as well as on *in situ* video, not quantified). The occurrence of large numbers of
552 ovigerous females, observed at the same period at two vent fields 300 km apart, and contrasting
553 with all previous collections along the nMAR (see 1985-2014 collection compilation, Table 4)

indicates that spawning activity varies temporally in *R. exoculata*, with a certain degree of synchrony at regional scale. Such pattern may possibly suggest spawning periodicity in *R. exoculata*. At this stage, additional observations are needed to assess its temporality, geographic extent, as well as possible drivers.

Table 4. Occurrence of brooding females in *Rimicaris exoculata* samples from different cruises on the nMAR since 1985.

Site	Jan	Feb	Mar	Apr	May	Jun	Jul	Aug	Sep	Oct	Nov	Dec
Rainbow 36°14'N						1998[5, 7]	1997[3] 2002[10]	2005[7]	2005[10]	1998[10]		
Broken Spur 29°10'N							1997[3] 2002[10]		1994[2,10] 1996[2, 10]			
TAG site 26°08'N	**2014***	**2014*** 2018[11]	2018[11]			2002[10]	1997[3]	1985[1] 2005[7]	1994[5]		2004[6]	
Snake Pit 23°22'N	**2014***	**2014*** 2018[11]	2018[11]			2002[10]	1997[3] 2001[7]	2003[10]			1995[7]	
Logatchev 14°45'N			2007[7-9]				1997[3,4] 2001[7]				1998[10]	

[1]Williams and Rona (1986), [2]Gebruk et al. (1997), [3]Shank et al. (1998), [4]Gebruk et al (2000), [5]Ramirez-Llodra et al. (2000), [6]Copley et al (2007), [7]Komai & Segonzac (2008), [8]Gebruk et al. (2010), [9]Guri et al. (2012), [10]Lunina and Vereshchaka (2014), [11]Methou et al. (2019), ***this study**. Reports included here examined several tens to several hundred specimens. Color code: blue: no brooding female reported; green: statement of "rare" brooding females or 1-2 brooding females reported; pink: statement of "many" brooding females or at least 10 brooding females in more quantitative reports.

Previous studies suggested continuous reproduction in *R. exoculata*, based on asynchronous ovarian development observed among females collected in summer at the Rainbow vent field and in autumn at TAG (Ramirez-Llodra et al. 2000, Copley et al. 2007). At that time, the lack of brooding females was explained by their migration out of dense aggregations towards areas with less exposure to harmful vent fluids to protect their eggs. Our observations suggest that brooding females actually remain in dense aggregations, but brooding activity may be restricted in time which could explain the lack of observations during other months. Additional

observations of ovarian development at different periods, taking into account the size of females, and perhaps also their distribution in the mixing gradient of vent fluid and seawater, are needed to better understand the gametogenic cycle of the species. In *Alvinocaris stactophila* from cold seeps in the Gulf of Mexico, females exhibit increasing oocyte size in gonads throughout the year, and ovigerous females are observed mainly in February-March (Copley and Young 2006). In *R. hybisae* from vents in the Cayman Trough, winter spawning was also suggested, but the effect of spatial population structure and need to expand temporal coverage was recognized (Nye et al. 2013). As for *R. hybisae*, we need to expand the temporal breath of observations on *R. exoculata* reproduction to better constrain its spawning seasonality and assess its degree of variability.

While most vent species along the MAR were suggested to reproduce continuously, seasonal spawning and recruitment was shown for *Bathymodiolus azoricus* mussels from the Menez Gwen vent field near the Azores (Colaço et al. 2006). The relatively shallow depth of Menez Gwen (850m), where the influence of seasonal phytoplankton variation is still significant compared to deeper sites provide a driver for this seasonality, as also suggested for *A. stactophila* at seeps of similar depth in the Gulf of Mexico (Copley and Young 2006). A sexual pause was observed in *Bathymodiolus puteoserpensis* occurring at sites below 2000m (Tyler and Young 1999), suggesting that seasonal spawning is also possible at depth, and that both environmental drivers and phylogenetic constraints may be important. In Alvinocarididae, both continuous and seasonal reproduction have been reported (Copley and Young, 2006, Ramirez-Llodra et al., 2000). In *R. exoculata*, polymodal size structures suggest discontinuous recruitment, which may also reflect periodic spawning. However, the effect of larval dispersal dynamics, recruitment temporality and post-settlement growth rates and mortality all remain to be assessed before any supported conclusion can be drawn.

4.2.2. Reproductive effort in R. exoculata at TAG and Snake Pit

597 Size at first reproduction represents a key life-history parameter reflecting the life-time
598 investment in reproduction of a species (Anger and Moreira 1998). In Alvinocaridid species, the
599 size at first reproduction varies between 50% (*R. hybisae*, Nye et al. 2013) and 60% (*A. muricola*,
600 Ramirez-Llodra and Segonzac 2006, *A. stactophila*, Copley and Young 2006, *M. fortunata*,
601 Ramirez-Llodra et al. 2000) of the maximal size of the species. *R. exoculata* thus falls within the
602 range of the family, with the smallest brooding females measuring 12 mm CL, which represents
603 50% of its maximal size. However, few females between 12 mm CL and 15 mm CL (i.e. < ESM)
604 were brooding eggs in our samples (3.5%) and likely represent 'premature' specimens, while
605 many more become sexually mature (36.5%) when they reach 15.1 mm CL (ESM), which
606 represents 62% of the species maximal size. Although a later onset of reproduction might limit life
607 time investment in reproduction for an iteroparous species (Ramirez-Llodra et al. 2000), favoring
608 reproduction to the largest individuals which produce the largest broods might be advantageous
609 and help to maximize energy investment in reproduction.

610 Fecundity in *R. exoculata* was on average of 833 eggs/female, ranging from 304 to 1879
611 eggs/female. This is in agreement with fecundities found in the few brooding females available
612 before our study (Ramirez-Llodra et al. 2000). In addition, *R. exoculata* fecundity is similar to that
613 reported for *R. hybisae* (max 1707 eggs/female, Nye et al. 2013), but lower than that of *R. chacei*
614 (2510 eggs for a female from Lucky Strike, Ramirez-Llodra et al. 2000). Egg sizes of *R. exoculata*
615 were consistent with those reported previously: 0.145 mm^3 for early stage eggs from TAG females
616 (Ramirez-Llodra et al. 2000), which is within the range reported here at similar stage (0.131-0.151
617 mm^3 at TAG and Snake Pit respectively). Other *Rimicaris* species have smaller eggs: 0.08 mm^3
618 for *R. hybisae* (Nye et al. 2013), and 0.09 mm^3 for *R. chacei* (Ramirez-Llodra et al. 2000). With
619 fecundities in the lower range of those reported for its genus, and eggs sizes in the upper range,
620 *R. exoculata* may have a specific strategy of higher parental investment per egg.

621 *R. exoculata* reproductive outputs differed between TAG and Snake Pit populations. Indeed
622 both realized fecundities and egg sizes were lower at TAG. Although we cannot completely
623 exclude a sampling effect on the observed fecundities at TAG, or variations in fertilization success
624 between vent fields, the difference in realized fecundity most probably reflects the larger body
625 sizes of brooding females at Snake Pit, and the positive allometric variation of fecundity with
626 female size. Similarly, differences in fecundity between *R. hybisae* females of two vent fields in
627 the Cayman Trough were primarily attributed to the large size differences observed between
628 shrimps of the two fields (Nye et al. 2013). The lower egg size at TAG, however, suggests that
629 additional factors, such as food availability or environmental challenges (fluid toxicity, temperature
630 stress), may also contribute to differences in reproductive investment between populations of the
631 two fields.

632 Both fields are at similar depth, 300 km apart along the ridge, and regional factors are
633 unlikely to provide environmental heterogeneity that could be linked to the different reproductive
634 investment. We hypothesize that local environmental factors associated with vent emissions are
635 more likely to affect *R. exoculata* reproductive effort. Shrimp tolerance to metallic elements and
636 dissolved gases in vent fluids depends on detoxification processes through metallothioneins,
637 antioxidants (Gonzalez-Rey et al. 2007) and metabolic activities of their symbiotic bacteria (Jan
638 et al. 2014, Cambon-Bonavita et al. 2021). Higher concentrations in some metallic elements in
639 hydrothermal fluids could force the shrimps to allocate more metabolic energy to detoxification
640 processes, at the expense of reproductive functions. TAG fluids have higher iron, copper and
641 manganese concentrations than those from Snake Pit (Desbruyères et al. 2000, Schmidt et al.
642 2008, Charlou et al. 2010), which could explain the lower reproductive output of shrimps at this
643 vent field. However, both bioenergetics and vent processes are complex and physiological
644 tolerance of reproductive shrimps must be experimentally tested (e.g. August et al. 2016), along
645 with a more detailed exploration of local vent chemistry.

4.3. Life history traits of *R. exoculata* males and females

Adult males and females of *R. exoculata* exhibit different distributions, which suggests distinct life history traits. Although spatial sex segregation is common in vent decapods, usually opposite trends have been reported, where males occupy areas closer to high temperature fluids or with steeper chemical gradients, whereas brooding females locate preferentially in areas with milder conditions (Perovitch et al. 2003, Copley and Young, 2006, Marsh et al. 2015).

4.3.1. Brooding in vent fluids

Brooding *R. exoculata* females were observed within dense aggregations at Logatchev (Gebruk et al. 2010, Guri et al. 2012). At TAG and Snake Pit, all brooding females we observed or collected were crawling in dense aggregations bathed in vent fluids. Only *R. hybisae* at vents in the Cayman Trough has also been observed brooding eggs in habitats exposed to hydrothermal influence (Nye et al. 2013).

Ovigerous females with broods at all developmental stages including hatching zoea were found in dense aggregations, suggesting that females of *R. exoculata* remain in areas exposed to vent fluids during the whole brooding period until they release the larvae. Exposure of embryos to high temperatures may accelerate their development and shorten the brooding period, while heat stress may also challenge normal development. *In vitro* incubations of embryos of *Shinkaicaris leurokolos*, an alvinocaridid species inhabiting vent areas exposed to hydrothermal fluids in Okinawa Trough, showed increased developmental rates with increasing temperature and optimal growth at temperatures within the range experienced by adults *in situ* (10-20°C, Watanabe et al. 2016). Embryos of *S. leurokolos* hatched within 9-12 weeks at 10°C and 3-4 weeks at 20°C (Watanabe et al. 2016). Considering the habitat of brooding females in *R. exoculata*, eggs are likely to hatch within a few weeks following spawning. Another observation in favor of a short brooding period is that ovigerous females did not appear to suffer excessive

mineral load on their carapace (FP personal observation). In *R. exoculata*, very frequent molting - every 10 days - may regularly eliminate mineral precipitations resulting from vent fluid exposure and overgrowing cephalothoracic symbiotic bacterial communities (Corbari et al. 2008). Since molting is interrupted during the brooding period in decapods (Correa and Thiel 2003), a long incubation within vent fluids would certainly result in highly mineralized cephalothoracic surfaces, which were not observed in our ovigerous females.

Brooding within vent fluids may also sustain the bacterial community observed on egg envelopes (Methou et al. 2019), and thus participate in symbiont transmission to the young shrimp through infestation of the larvae (Hernandez Avila et al. 2015, Methou et al. 2019). Another speculative hypothesis would be that mothers could imprint their offspring with vent signature by bathing their eggs within vent fluids during embryonic development, which would later help them return to suitable vent habitats after dispersal. Such homing process might involve the strongly developed higher brain centers of *R. exoculata* enabling the memory and navigation skills necessary to locate suitable recruitment sites (Machon et al. 2019), as well as their sensory abilities to detect vent environments (Ravaux et al. 2021).

4.3.2. Mating in the periphery

At TAG, half of the males of our sampling set were collected in the inactive periphery, suggesting that they spend a significant part of their time there, and raising questions on the underlying driving factors. It is unlikely that males stay permanently at the periphery because they need to supply their symbiotic bacteria with reduced compounds of the vent fluids to ensure their nutrition (Ponsard et al. 2013). Alternative diet on food items (particles, microbial mats) picked on the substratum in inactive areas is unlikely because the morphology of their cephalothorax and chelipeds is not suited for such feeding strategy (Segonzac et al. 1993). Peripheral areas also harbor more predators, such as *Maractis rimicarivora* anemones (Fautin and Barber 1999, Copley

694 et al. 2007) that are excluded from dense aggregations where environmental conditions are
695 probably too harsh. The migration of *R. exoculata* males to inactive areas is therefore not likely
696 driven by trophic needs and expose individuals to increased predatory risk. The hypothesis of a
697 reproductive behavior remains a plausible explanation. In Caridean shrimps, females molt before
698 egg extrusion, and mating occurs following this pre-spawning molt (Bauer 2004). Vent shrimps
699 may migrate briefly towards a milder habitat for molting to avoid exposure to vent fluids while they
700 are most vulnerable. Location in peripheral areas might be advantageous for males to reach
701 females just after their pre-spawning molt and mate successfully.

702 In crustaceans, body sizes and male weaponery have been associated with the mating
703 system (Correa & Thiel 2003, Baeza & Thiel 2007, Asakura 2009). In free-living caridean shrimps,
704 larger males are usually observed in mating systems that involve sexual competition for females
705 or precopulatory mate guarding (Bauer 1996, Correa & Thiel 2003, Asakura 2009). In contrast,
706 the lack of sexual competition in “pure searching” mating systems or long-term mate (monogamy
707 or semi-monogamy) is generally associated with similar or smaller-sized males (Bauer 1996,
708 Correa & Thiel 2003). In *R. exoculata*, sexually mature females, i.e. those actually involved in the
709 courtship and mating processes, have similar or slightly larger sizes than males. In addition, *R.*
710 *exoculata* lacks sexual dimorphism in secondary characters associated with male competition
711 (e.g. increase in cheliped size and cephalotorax). Thus, a “pure searching” model where males
712 search for receptive females just after their reproductive molt using mostly tactile signals or
713 pheromones (Bauer 1976, 1996) could better describe the mating system in *R. exoculata*. In
714 several instances, we observed *R. exoculata* pairs at the periphery of dense shrimp aggregations,
715 with a male (supposedly) clutching a female (sometimes identified by its pink dorsal gonads) with
716 its walking legs (Video S1 AppendixB-C). Such behavior is typical of the mating process described
717 by Bauer (1976) for *Heptocarpus pictus*, a caridean shrimp exhibiting a “pure searching” mating
718 model.

4.4. A life-history scenario for *Rimicaris* shrimps at vents

Our observations on the distribution of the sexes and life-stages of *R. exoculata* at vents, and our hypotheses on the drivers of these distributions can be synthesized in a possible life-history scenario (Fig. 6). Juveniles appear to settle directly among their older conspecifics, in areas bathed with hydrothermal fluids, forming patches within dense aggregations, and thus contributing to the heterogeneity of these assemblages. Such gatherings of juveniles might be the result of discrete settlement events and/or reflect different tolerance or physiological needs of new settlers compared to those of older individuals. After settlement, *R. exoculata* juveniles remain in dense aggregations where they grow to the subadult and adult stages. When they reach sexual maturity, adults could migrate in less active parts of vent fields for mating and spawning. Sexually mature males would reach a position where they could “more easily” encounter sexually receptive females that move at the periphery for their pre-spawning molt. After mating and egg extrusion, females would return to dense aggregations to brood their eggs, while the fate of males remains uncertain. Males may however return to dense aggregations at some point to fulfill their nutrition needs. After an incubation period of a few weeks on chimney walls, brooding females would release zoea larvae (Hernández-Ávila et al. 2015). These larvae would disperse within bathypelagic waters, developing and feeding for a while on pelagic food items until they reach a large post-larval stage and return to a benthic and chemosynthetic life style at vents. The benthic life of the conspecific *R. chacei* may follow a different scenario as settlement occurs in the herein so-called nurseries that form a distinct habitat from that of *R. exoculata*. Further observations by Methou et al. (2022) indeed highlight a different post-settlement trajectory resulting in much smaller adult populations for this species.

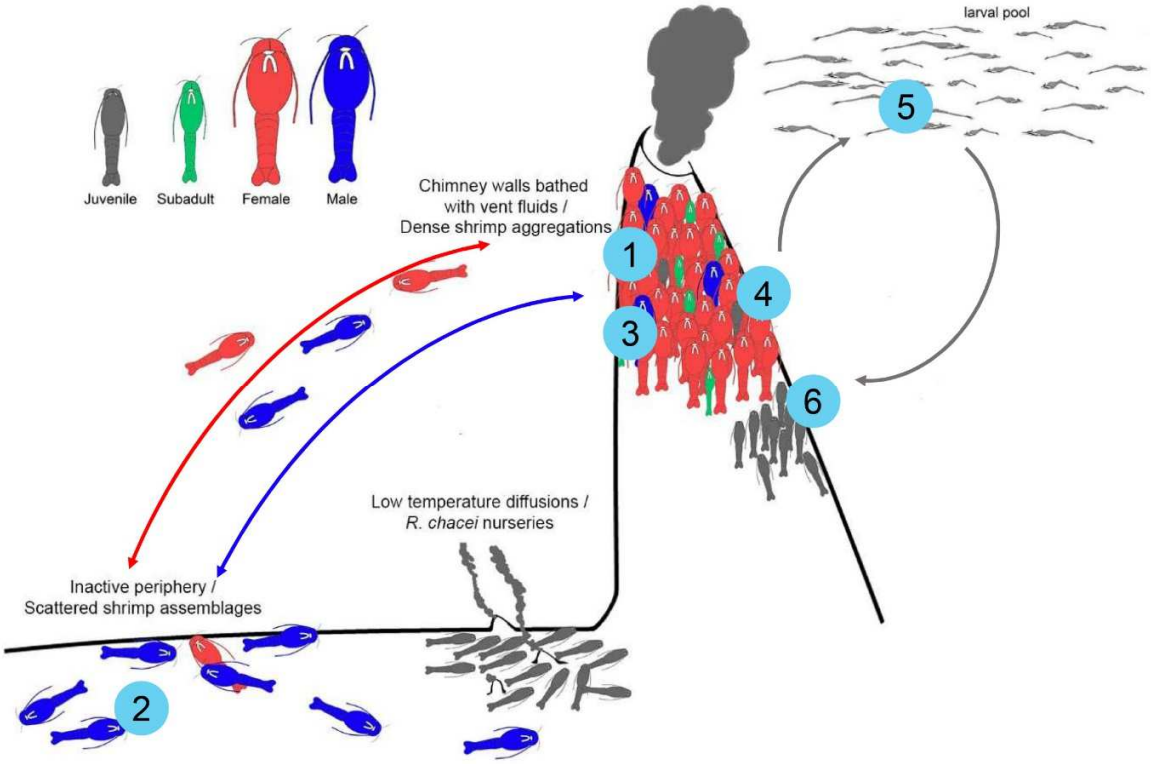

Life stage	Habitat	Observation	Reference
1 Growth & maturation	Chimney walls	All stages from juveniles to adults are present, few males.	This study.
2 Mating & spawning	Periphery	Many adult males, rare females, mating behavior observed.	This study.
3 Brooding	Chimney walls	Brooding females with embryos at all stages.	Guri et al. 2012, this study.
4 Larvae release	Chimney walls	Late broods and hatched females are present, zoe larvae collected near adult populations.	Hernandez-Avila et al. 2015, this study.
5 Larval dispersal	Bathypelagic	*Rimicaris* post-larval stages collected 200-1000 m above vents.	Herring & Dixon 1998
6 Recruitment	Chimney walls	Most juveniles observed in dense aggregations.	Methou et al. 2020, this study.

Figure 6. Schematic scenario depicting life history and habitat use of *Rimicaris exoculata* through its life cycle at vents on the nMAR.

5. Conclusion

This study revealed complex population structures in *R. exoculata*, with spatial variations in life-stage distributions between and within visually distinct shrimp assemblages of a single vent field. This complexity is probably the result of habitat heterogeneity at small spatial scales and different physiological and nutritional requirements along the shrimp life cycle. Males and females contrasting spatial distributions resulted in strongly biased sex ratios locally, and could be related to their reproductive strategy involving mating at the periphery of dense aggregations and incubation of the eggs within vent fluids.

The physiological and nutritional flexibility allowing male holobionts to cope with conditions that may be deleterious for their symbiotic communities remains to be assessed. Spatial distributions of the early stages, reflecting changes in their physiological tolerance and/or resource use, are also probably related to symbiont proliferation and their gradual transition towards a chemosynthetically derived nutrition. A more detailed analysis of the interplay between environmental conditions, shrimp life stages as well as the development of their symbiotic community as they grow is needed to better understand the factors driving the observed *in situ* distributions.

Finally, future studies should provide insights into temporal stability of the spatial patterns we observed. In particular, temporal variability in reproductive activity needs a more thorough assessment through repeated observations at our study sites and other vents along the mid-Atlantic ridge. Such studies are required to accurately estimate seasonally in reproduction of deep-sea species, and identify the underlying drivers.

Credit author statement:

Iván Hernández-Ávila : Conceptualization, methodology, formal analysis, investigation, writing – original draft.

Marie-Anne Cambon-Bonavita : Resources, supervision, writing – review & editing.

Jozée Sarrazin : Resources, writing – review & editing.

Florence Pradillon : Conceptualization, methodology, resource, supervision, writing – review & editing.

Acknowledgment

This research was supported by Ifremer REMIMA program, EU Seventh Program for Research, Technological Development and Demonstration Activities, MIDAS grant 603418, FGMA PhD grant E-223-85-2012-2 to IHA and Campus France grant 796045K to IHA. We also thank the captain and crew of the oceanographic cruise BICOSE-2014 (DOI: 10.17600/14000100), as well as the pilots of the ROV Victor 6000. We also thank M. Segonzac for his help on juvenile sorting during the BICOSE cruise.

References

Anger K, Moreira GS (1998) Morphometric and reproductive traits of tropical caridean shrimps. Journal of Crustacean Biology 18: 823-838, doi: 10.1163/193724098X00674.

Asakura A (2009) The evolution of mating systems in decapod crustaceans. In: Martin JW, Crandall KA, Felder DL (eds) Decapod crustacean phylogenetics. CRC Press.

790 Auguste M, Mestre NC, Rocha TL, Cardoso C, Cueff-Gauchard V, Le Bloa S, Cambon-
791 Bonavita M-A, Shillito B, Zbinden M, Ravaux J, Bebianno MJ (2016) Development of an
792 ecotoxicological protocol for the deep-sea fauna using the hydrothermal vent shrimp *Rimicaris*
793 *exoculata*. Aquatic Toxicology 175: 277-285. doi: 10.1016/j.aquatox.2016.03.024.
794 Baeza JA, Thiel M (2007) The mating system of symbiotic crustaceans: a conceptual
795 model based on optimality and ecological constraints. In: Duffy JE, Thiel M (eds) Evolutionary
796 ecology of social and sexual systems: Crustaceans as a model organisms. Oxford University
797 Press.
798 Bauer RT (1996) A test of hypotheses on male mating systems and female molting in
799 decapod shrimp, *Sicyonia dosalis* (Decapoda: Penaeoidea). Journal of Crustacean Biology
800 16:429-436, doi: 10.2307/1548731.
801 Bauer, RT (1976) Mating behaviour and spermatophore transfer in the shrimp
802 *Heptacarpus pictus* (Stimpson) (Decapoda: Caridea: Hippolitidae). Journal of Natural History 10:
803 415-440.
804 Bauer RT (2004) Chapter 6: Reproductive biology. In: Remarkable shrimps: adaptations
805 and natural history of the carideans. Pp 111-136. University of Oklahoma press.
806 Beedessee G, Watanabe H, Ogura T, Nemoto S, Yahagi T, Nakagawa S, Nakamura K,
807 Takai K, Koonjul M, Marie DEP (2013) High connectivity of animal populations in deep-sea
808 hydrothermal vent fields in the Central Indian Ridge relevant to its geological setting. PLoS One
809 8:e81570, doi: 10.1371/journal.pone.0081570.
810 Cambon-Bonavita M-A, Aubé J, Cueff-Gauchard V, Reveillaud J (2021). Niche partitioning
811 in the Rimicaris exoculata holobiont : the case of the first symbiotic Zetaproteobacteria.
812 Microbiome 9:87, doi: 10.1186/s40168-021-01045-6
813 Charlou J-L, Donval J-P, Konn C, Ondreas H, Fouquet Y, Jean-Baptiste P, Fourre E
814 (2010) High production and fluxes of H_2 and CH_4 and evidence of abiotic hydrocarbon synthesis
815 by serpentinization in ultramafic-hosted hydrothermal systems on the Mid-Atlantic Ridge. In

816 Diversity of Hydrothermal Systems on Slow-spreading Ocean Ridges. Geophysical Monograph
817 Series 188: 265-296.
818 Colaço A, Martins I, Laranjo M, Pires L, Leal C, Prieto C, Costa V, Lopes H, Rosa D,
819 Dando PR, Serrao-Santos R (2006) Annual spawning of the hydrothermal vent mussel,
820 *Bathymodiolus azoricus*, under controlled aquarium, conditions at atmospheric pressure. Journal
821 of Experimental Marine Biology and Ecology 333:166-171, doi:10.1016/j.jembe.2005.12.005.
822 Copley JTP, Jorgensen PBK, Sohn RA (2007) Assessment of decadal-scale ecological
823 change at a deep Mid-Atlantic hydrothermal vent and reproductive time-series in the shrimp
824 *Rimicaris exoculata*. Journal of the Marine Biological Association of the United Kingdom 87:859-
825 867, doi: 10.1017/S0025315407056512.
826 Copley JTP, Tyler PA, Murton BJ, Van Dover CL (1997) Spatial and interannual variation
827 in the faunal distribution at Broken Spur vent field (29°N, Mid-Atlantic Ridge). Marine Biology
828 129:723-733, doi : 10.1007/s002270050215.
829 Copley JTP, Tyler PA, Van Dover CL, Schultz A, Dickson P, Singh S, Sulanowska M
830 (1999) Subannual temporal variation in faunal distributions at the TAG hydrothermal mound (26°
831 N, Mid-Atlantic Ridge). Marine Ecology 20:291-306, doi: 10.1046/j.1439-0485.1999.2034076.x.
832 Copley JTP, Young CM (2006) Seasonality and zonation in the reproductive biology and
833 population structure of the shrimp *Alvinocaris stactophila* (Caridea: Alvinocarididae) at a Louisiana
834 Slope cold seep. Marine Ecology Progress Series 315:199-209, doi: 10.3354/meps315199.
835 Corbari L, Zbinden M, Cambon-Bonavita M-A, Gaill F, Compère P (2008) Bacterial
836 symbionts and mineral deposits in the branchial chamber of the hydrothermal vent shrimp
837 *Rimicaris exoculata*: relationship to moult cycle. Aquatic Biology, 1:225-238, doi:
838 10.3354/ab00024.
839 Correa C, Thiel M (2003) Mating systems in caridean shrimp (Decapoda: Caridea) and
840 their evolutionary consequences for sexual dimorphism and reproductive biology. Revista Chilena
841 de Historia Natural, 76(2): 187-203, doi: 10.4067/S0716-078X2003000200006.

842 Cuvelier D, Legendre P, Laes A, Sarradin PM, Sarrazin J (2014) Rhythms and community
843 dynamics of a hydrothermal tubeworm assemblage at Main Endeavour Field – A multidisciplinary
844 deep-sea observatory approach. PLoS ONE 9(5): e96924, doi: 10.1371/journal.pone.0096924.
845 Cuvelier D, Sarrazin J, Colaco A, Copley J, Desbruyeres D, Glover AG, Tyler P, Serrao
846 Santos R (2009) Distribution and spatial variation of hydrothermal faunal assemblages at Lucky
847 Strike (Mid-Atlantic Ridge) revealed by high-resolution video image analysis. Deep Sea Research
848 I 56: 2026-2040, doi: 10.1016/j.dsr.2009.06.006.
849 Cuvelier D, Sarrazin J, Colaço A, Copley JT, Glover AG, Tyler PA, Santos RS,
850 Desbruyères D (2011) Community dynamics over 14 years at the Eiffel Tower hydrothermal
851 edifice on the Mid-Atlantic Ridge. Limnology & Oceanography 56(5): 1624-1640, doi:
852 10.4319/lo.2011.56.5.1624.
853 Desbruyères D, Almeida A, Biscoito M, Comtet T, Khripounoff A, Le Bris N, Sarradin PM,
854 Segonzac M (2000) A review of the distribution of hydrothermal vent communities along the
855 northern Mid-Atlantic Ridge: dispersal vs. environmental controls. Hydrobiologia 440: 201-216,
856 doi: 10.1023/A:1004175211848.
857 Desbruyères D, Biscoito M, Caprais JC, Colaço A, Comtet T, Crassous P, Fouquet Y,
858 Khripounoff A, Le Bris N, Olu K, Riso R, Sarradin PM, Segonzac M, Vangriesheim A (2001)
859 Variations in deep-sea hydrothermal vent communities on the Mid-Atlantic Ridge near the Azores
860 plateau. Deep Sea Research I 48: 1325-1346, doi: 10.1016/S0967-0637(00)00083-2.
861 Doyle JJ (1990) Isolation of plant DNA from fresh tissue. Focus 12: 13-15.
862 Edgar RC (2004) MUSCLE: multiple sequence alignment with high accuracy and high
863 throughput. Nucleic Acids Research 32(5): 1792-1797, doi: 10.1093/nar/gkh340.
864 Fautin DG, Barber BR (1999) *Maractis rimicarivora*, a new genus and species of sea
865 anemone (Cnidaria: Anthozoa: Actinaria: Actinostolidae) from the Atlantic hydrothermal vent.
866 Proceedings of the Biological Society of Washington 112: 624-631.

867 Folmer O, Black M, Hoeh W, Lutz RA, Vrijenhoek RC (1994) DNA primers for amplification
868 of mitochondrial cytochrome c oxidase subunit I from diverse metazoan invertebrates. Molecular
869 Marine Biotechnology 3: 294-299.
870 Gebruk AV, Chevaldonné P, Shank T, Lutz RA, Vrijenhoek RC (2000) Deep-sea
871 hydrothermal vent communities of the Logatchev area (14°45'N, Mid-Atlantic Ridge): diverse
872 biotopes and high biomass. Journal of the Marine Biological Association of the United Kingdom
873 80(3): 383-393, doi: 10.1017/S0025315499002088.
874 Gebruk AV, Fabri M-C, Briand P, Desbruyeres D (2010) Community dynamics over a
875 decadal scale at Logatchev, 14°42´N, Mid-Atlantic Ridge. Cahiers de Biologie Marine 51: 383-
876 388, doi: 10.21411/CBM.A.FB805CDE.
877 Gebruk AV, Galkin SV, Vereshchaka AL, Moskalev LI, Southward AJ (1997) Ecology and
878 biogeography of the hydrothermal vent fauna of the Mid-Atlantic Ridge. Advances in Marine
879 Biology 32(32): 92-144, Doi: 10.1016/S0065-2881(08)60016-4.
880 Gonzalez-Rey M, Serafim A, Company R, Bebianno MJ (2007) Adaptation to metal
881 toxicity: a comparison of hydrothermal vent and coastal shrimps. Marine Ecology 28: 100-107,
882 doi: 10.1111/j.1439-0485.2006.00126.x.
883 Guri M, Durand L, Cueff-Gauchard V, Zbinden M, Crassous P, Shillito B, Cambon-
884 Bonavita M-A (2012) Acquisition of epibiotic bacteria along the life cycle of the hydrothermal
885 shrimp *Rimicaris exoculata*. ISME J 6: 597-609, doi: 10.1038/ismej.2011.133.
886 Hernández-Ávila I, Cambon-Bonavita M-A, Pradillon F (2015) Morphology of first zoeal
887 stage of four genera of alvinocaridid shrimps from hydrothermal vents and cold seeps:
888 Implications for ecology, larval biology and phylogeny. PLoS ONE 10(12): e0144657, doi:
889 10.1371/journal.pone.0144657.
890 [Dataset] Hernandez Avila I, Cambon Bonavita M-A, Sarrazin J, Pradillon F (2021)
891 Demographic and reproduction data of hydrothermal vent alvinocaridid shrimps collected on the
892 Mid Atlantic Ridge during the Bicose cruise (2014). SEANOE. https://doi.org/10.17882/84112

893 Herring PJ, Dixon DR (1998) Extensive deep-sea dispersal of postlarval shrimp from a
894 hydrothermal vent. Deep-Sea Research I 45: 2105-2118, doi: 10.1016/S0967-0637(98)00050-8.
895 Husson B, Sarradin P-M, Zeppilli D, Sarrazin J (2017) Picturing thermal niches and
896 biomass of hydrothermal vent species. Deep-Sea Research II 137: 6-25, doi:
897 10.1016/j.dsr2.2016.05.028
898 Jan C, Petersen JM, Werner J, Teeling H, Huang S, Glöckner FO, Golyshina OV, Dubilier
899 N, Golyshin PN, Jebbar M, Cambon-Bonavita M-A (2014) The gill chamber epibiosis of deep-sea
900 shrimp *Rimicaris exoculata*: an in-depth metagenomic investigation and discovery of
901 *Zetaproteobacteria*. Environmental Microbiology 16: 2723-2738, doi:10.1111/1462-2920.12406.
902 Kearse M, Moir R, Wilson A, Stones-Havas S, Cheung M, Sturrock S, Buxton S, Cooper
903 A, Markowitz S, Duran C, Thierer T, Ashton B, Meintjes P, Drummond A (2012) Geneious Basic:
904 an integrated and extendable desktop software platform for the organization and analysis of
905 sequence data. Bioinformatics 28(12): 1647–9, doi: 10.1093/bioinformatics/bts199.
906 Komai T, Segonzac M (2008) Taxonomic review of the hydrothermal vent shrimp genera
907 *Rimicaris* Williams & Rona and *Chorocaris* Martin & Hessler (Crustacea: Decapoda: Caridea:
908 Alvinocarididae). Journal of Shellfish Research 27(1): 21-41, doi: 10.2983/0730-
909 8000(2008)27[21:TROTHV]2.0.CO;2.
910 Le Bloa S, Boidin-Wichlacz C, Cueff-Gauchard V, Rosa RD, Cuvillier-Hot V, Durand L,
911 Methou P, Pradillon F, Cambon-Bonavita MA, Tasiemski A (2020) Antimicrobial peptides and
912 ectosymbiotic relationships: involvement of a novel type IIa crustin in the life cycle of a deep-sea
913 vent shrimp. Frontiers in Immunology 11: 1511, doi: 10.3389/fimmu.2020.01511.
914 Lunina A, Vereshchaka A (2014) Distribution of hydrothermal alvinocaridid shrimps: effect
915 of geomorphology and specialization to extreme biotopes. PLoS ONE 9(3): e92802, doi:
916 10.1371/journal.pone.0092802.
917 MacDonald P (2003) The mixdist package – MIX for the R Environment.

Machon J, Krieger J, Meth R, Zbinden M, J Ravaux, N Montagné, Chertemps T, Harzsh S (2019) Neuroanatomy of a hydrothermal vent shrimp provides insights into the evolution of crustacean brain centers. eLife 8: e47550, doi.org/10.7554/eLife.47550.

Marsh L, Copley JT, Tyler PA, Thatje S (2015) In hot and cold water: differential life-history traits are key to success in contrasting thermal deep-sea environments. Journal of Animal Ecology 84: 898-913, doi: 10.1111/1365-2656.12337.

McGuinness KA (2002) Of rowing boats, ocean liners and tests of the ANOVA homogeneity of variance assumption. Austral Ecology 27: 681-688, doi: 10.1046/j.1442-9993.2002.01233.x.

Methou P, Hernandez-Avila I, Aube J, Cueff-Gauchard V, Gayet N, Amand L, Shillito B, Pradillon F, Cambon-Bonavita M-A (2019) Is it first the egg of the shrimp? – Diversity and variation in microbial communities colonizing broods of the vent shrimp *Rimicaris exoculata* during embryonic development. Frontiers in Marine Science 10:808, doi: 10.3389/fmicb.2019.00808.

Methou P, Michel LN, Segonzac M, Cambon-Bonavita M-A, Pradillon F (2020) Integrative taxonomy revisits the ontogeny and trophic niches of *Rimicaris* vent shrimps. Royal Society Open Science 7: 200837, doi: 10.1098/rsos.200837.

Methou P, Hernandez-Avila I, Cathalot C, Cambon-Bonavita M-A, Pradillon F (2022) Population structure and environmental niches of Rimicaris shrimps from the Mid-Atlantic Ridge. Marine Ecology Progress Series 684: 1-20, doi: 10.3354/meps13986.

Nye V, Copley JT, Tyler PA (2013). Spatial Variation in the Population Structure and Reproductive Biology of *Rimicaris hybisae* (Caridea: Alvinocarididae) at Hydrothermal Vents on the Mid-Cayman Spreading Centre. PLoS ONE 8(3): e60319, doi:10.1371/journal.pone.0060319.

Oh CW, Hartnoll RG (2004) Reproductive biology of the common shrimp *Crangon crangon* (Decapoda: Crangonidae) in the central Irish Sea. Marine Biology 144: 303-316, doi: 10.1007/s00227-003-1205-6.

943 Perovich GM, Epifanio CE, Dittel AI, Tyler PA (2003) Spatial and temporal patterns in
944 development of eggs in the vent crab *Bythograea thermydron*. Marine Ecology Progress Series
945 251: 211-220, doi: 10.3354/meps251211.
946 Ponsard J, Cambon-Bonavita M-A, Zbinden M, Lepoint G, Joassin A, Corbari L, Shillito B,
947 Durand L, Cueff-Gauchard V, Compere P (2013) Inorganic carbon fixation by chemosynthetic
948 ectosymbionts and nutritional transfers to the hydrothermal vent host-shrimp *Rimicaris exoculata*.
949 ISME J 7: 96-109, doi:10.1038/ismej.2012.87.
950 R Development Core Team (2008). R: A language and environment for statistical
951 computing. R Foundation for Statistical Computing, Vienna, Austria. ISBN 3-900051-07-0.
952 Ramirez-Llodra E, Tyler PA, Copley JTP (2000) Reproductive biology of three caridean
953 shrimp, *Rimicaris exoculata*, *Chorocaris chacei* and *Mirocaris fortunata* (Caridea: Decapoda),
954 from hydrothermal vents. Journal of the Marine Biological Association of the United Kingdom 80:
955 473-484.
956 Ramirez-Llodra E, Segonzac M (2006) Reproductive biology of *Alvinocaris muricola*
957 (Decapoda: Caridea: Alvinocarididae) from cold seeps in the Congo Basin. Journal of the Marine
958 Biological Association of the United Kingdom 86: 1347-1356, doi: 10.1017/S0025315406014378.
959 Ravaux J, Léger N, Hamel G, Shillito B (2019) Assessing a species thermal tolerance
960 through a multiparameter approach : the case study of the deep-sea vent shrimp *Rimicaris*
961 *exoculata*. Cell Stress and Chaperones 24: 647-659, doi: 10.1007/s12192-019-01003-0.
962 Ravaux J, Machon J, Shillito B, Barthélémy D, Amand L, Cabral M, Delcour E, Zbinden M
963 (2021) Do hydrothermal shrimp smell vents? Insects 12, 1043, doi: 10.3390/insects12111043.
964 Sarrazin J, Legendre P, de Busserolles F, Fabri M-C, Guilini K, Ivanenko VN, Morineaux
965 M, Vanreusel A, Sarradin PM (2015) Biodiversity patterns, environmental drivers and indicator
966 species on a high-temperature hydrothermal edifice, Mid-Atlantic Ridge. Deep Sea Research II:
967 121: 177-192, doi: 10.1016/j.dsr2.2015.04.013.

968 Sarrazin J, Robigou V, Juniper SK, Delaney JR (1997) Biological and geological evolution
969 over four years on a high temperature hydrothermal vent structure, Juan de Fuca Ridge. Marine
970 Ecology Progress Series 153: 5-24, doi: 10.3354/meps153005.
971 Schmidt C, Le Bris N, Gaill F (2008) Interactions of deep-sea vent invertebrates with their
972 environment: The case of *Rimicaris exoculata*. Journal of Shellfish Research 27: 79-90, doi:
973 10.2983/0730-8000(2008)27[79:IODVIW]2.0.CO;2.
974 Segonzac M, de Saint Laurent M, Casanova B (1993) L'énigme du comportement
975 trophique des crevettes Alvinocarididae des sites hydrothermaux de la dorsale médio-atlantique.
976 Cahier de Biologie Marine 34: 535-571.
977 Shank TM, Lutz RA, Vrijenhoek RC (1998) Molecular systematics of shrimp (Decapoda:
978 Bresiliidae) from deep-sea hydrothermal vents, I: Enigmatic "small orange" shrimp from the Mid-
979 Atlantic Ridge are juvenile *Rimicaris exoculata*. Molecular Marine Biotechnology 7: 88-96.
980 Teixeira S, Serrão EA, Arnaud-Haond S (2012) Panmixia in a fragmented and unstable
981 environment: the hydrothermal shrimp *Rimicaris exoculata* disperses extensively along the Mid-
982 Atlantic Ridge. PLoS ONE 7(6): e38521, doi:10.1371/journal.pone.0038521.
983 Thaler AD, Zelnio K, Saleu W, Schultz TF, Carlsson J, Cunningham C, Vrijenhoek RC,
984 Van Dover CL (2011) The spatial scale of genetic subdivision in populations of *Ifremeria nautilei*,
985 a hydrothermal-vent gastropod from the southwest Pacific. BMC Evolutionary Biology 11: 372,
986 doi.org/10.1186/1471-2148-11-372.
987 Tyler P A, Young C M (1999) Reproduction and dispersal at vents and cold seeps. Journal
988 of the Marine Biological Association of the United Kingdom 79: 193-208, doi:
989 10.1017/S0025315499000235.
990 Underwood AJ (1997) Experiments in ecology, their logical design and interpretation using
991 Analysis of Variance. Cambridge University Press, Cambridge.

992 Van Dover C L (2014) Impacts of anthropogenic disturbances at deep-sea hydrothermal
993 vent ecosystems: A review. Marine Environmental Research 102: 59-72, doi:
994 10.1016/j.marenvres.2014.03.008.
995 Van Dover C L, Arnaud-Haond S, Gianni M, Helmreich S, Huber J A, Jaeckel A L, Metaxas
996 A, Pendleton L H, Petersen S, Ramirez-Llodra E, Steinberg P E, Tunnicliffe V, Yamamoto (2018)
997 Scientific rationale and international obligations for protection of active hydrothermal vent
998 ecosystems from deep-sea mining. Marine Policy 90: 20-28, doi: 10.1016/j.marpol.2018.01.020.
999 Vereshchaka AL (1997) Comparative morphological studies on four populations of the
1000 shrimp *Rimicaris exoculata* from the Mid-Atlantic Ridge. Deep Sea Research I 44(11): 1905-1921,
1001 doi: 10.1016/S0967-0637(97)00031-9.
1002 Watanabe H, Yahagi T, Nagai Y, Seo M, Kojima S, Ishibashi J, Yamamoto H, Fujikura K,
1003 Mitarai S, Toyofuku T. 2016. Different thermal effects for brooding and larval dispersal of two
1004 neighboring distributed shrimps in a deep-sea hydrothermal vent field. Marine Ecology 37: 1282-
1005 1289, doi:10.1111/maec.12318.
1006 Williams AB, Rona PA (1986) Two new caridean shrimps (Bresiliidae) from a hydrothermal
1007 field on the Mid-Atlantic Ridge. Journal of Crustacean Biology 6(3): 446-462, doi:
1008 10.2307/1548184.
1009 Zar JH (2010) Biostatistical Analysis. Prentice Hall.
1010 Zbinden M, Berthod C, Montagné N, Machon J, Léger N, Chertemps T, Rabet N, Shillito
1011 B, Ravaux J (2017) Comparative study of chemosensory organs of shrimps from hydrothermal
1012 vent and coastal environments. Chemical Senses 42: 319-331, doi: 10.1093/chemse/bjx007.
1013 Zbinden M & Cambon-Bonavita MA (2020) *Rimicaris exoculata* : biology and ecology of a
1014 shrimp from deep-sea hydrothermal vents associated with ectosymbiotic bacteria. Marine
1015 Ecology Progress Series 652: 187-222, doi: 10.3354/meps13467.